BULGARIAN ACADEMY OF SCIENCES

INSTITUTE OF MICROBIOLOGY

“STEPHAN ANGELOFF”

Eng. Saveta Georgieva Mladenova

Investigation of the anti-obesogenic potential of extracts from *Alchemilla monticola* Opiz and *Ononis spinosa* L. towards the control of obesity in *in vitro* and *in vivo* models

SUMMARY

On a dissertation

for the award of educational and scientific

degree of ‘Doctor’ in the field of 5.11. Biotechnology

(Technology of biologically active molecules)

Scientific supervisor: Prof. Dr Milen I. Georgiev

Plovdiv, 2026

The dissertation comprises 108 pages and is illustrated with 24 figures and 7 tables. A total of 223 literature sources are cited.

The dissertation has been approved and scheduled for defense by the National Scientific Seminar in “Applied Microbiology and Microbial Biotechnologies” at the Institute of Microbiology “Stefan Angeloff”, Bulgarian Academy of Sciences. The seminar session was held on June 19, 2026.

The PhD candidate was granted the right to defend the dissertation by Order No. I-81/28.05.2026, issued by the Director of the Institute of Microbiology, BAS, prof. Penka Petrova, DSc.

Members of the scientific jury:

Prof. Dr. Svetla Danova

Assoc. Prof. Dr. Petya Dimitrova

Prof. Dr. Velizar Kostadinov Gochev

Prof. Dr. Magdalena Kondeva-Burdina

Prof. Dr. Teodora Svetoslavova Handjieva-Darlenska

The dissertation defense will take place at ..... from ..... hours in the seminar hall of the Institute of Microbiology “Stephan Angeloff” – BAS (IMikB), Sofia, Bulgaria.

The defense materials are available at IMikB – BAS and are published on the IMikB – BAS website.

Contents:

Abbreviations used

ACC	Acetyl-CoA carboxylase
ADIPOQ	Adiponectin
AKT	Protein kinase B
ALM	Extract of *A. monticola*
AMPK	Adenosine monophosphate-activated protein kinase
AST	Astragalin
ATP	Adenosine triphosphate
CEBP	CAAT/enhancer-binding protein
CTCF	Corrected total cell fluorescence
DMSO	Dimethyl sulfoxide
DNA	Deoxyribonucleic acid
ER	Estrogen receptor
FASN	Fatty acid synthase
GAPDH	Glyceraldehyde-3-phosphate dehydrogenase
IGF	Insulin-like growth factor
INSR	Insulin receptor
IRS	Insulin receptor substrate
MACK	maackiain
MSCs	Mesenchymal stem cells
MTT	3-(4,5-dimethylthiazol-2-yl)-2,5-diphenyltetrazolium bromide
ONON	Ononin
OSR	Extract of *O. spinosa*
ORST	Orlistat
PI3K	Phosphoinositide 3-kinase
PPAR	Peroxisome proliferator-activated receptor
QUE	Quercitrin
RNA	Ribonucleic acid
RPL13A	Ribosomal protein L13a
RT-qPCR	Quantitative real-time polymerase chain reaction
SERBP	Sterol regulatory element-binding protein
SGBS	Simpson-Golabi-Behmel syndrome
SIRT	Sirtuin
TUBB	Tubulin
WB	Western blot
NMR	Nuclear magnetic resonance spectroscopy

I. INTRODUCTION

The use of medicinal plants has a centuries-long history, including for weight control, based mainly on empirical ethnopharmacological knowledge (Vasileva et al., 2018; Anyanwu et al., 2025). The multi-component composition of plant extracts and the complex structure of the secondary metabolites they contain contribute to the synergistic effect in the treatment of obesity (Atanasov et al., 2021; Vasileva et al., 2020a). Deciphering the mechanism of action of medicinal plants using modern approaches such as metabolomics, transcriptomics and proteomics may accelerate the discovery of new bioactive compounds effective against obesity (Park et al., 2016; Georgiev et al., 2020; Zaghlool et al., 2021). The most important advantage of natural products is that their action is exerted by influencing more than one molecular mechanism.

In recent years, there has been a trend towards an increase in the prevalence of obesity and related diseases. According to estimates by the World Health Organisation (WHO), there are more than 650 million people worldwide who are obese, defined as having a body mass index (BMI) of over 30 kg/m² (Kivimaki et al., 2022). Forecasts for global levels of high BMI indicate that nearly 3.3 billion adults could be affected by 2035, compared to 2.2 billion in 2020. This represents an increase of over 54% by 2035. For young people aged 5 to 19, the value rises from 22% with high BMI (430 million) to over 39% (770 million) over the next decade (World Obesity Federation, 2024).

Excessive fat accumulation in obesity has a multifactorial etiology, but energy imbalance in the body plays a key role. As a result, excess calories are stored as a triglycerides in adipose tissue. In addition to energy imbalance, impaired functioning of the central nervous system—which is responsible for the fine regulation of energy expenditure *via* neural and humoral mechanisms, as well as the homeostasis of adipose tissue—contributes to the development of obesity and its associated diseases.

Obesity has a significant impact on quality of life, even in clinically healthy individuals. Despite public health policies and individual efforts to combat it, over 2 billion people worldwide are affected by this health problem. Clearly, the identification of genetic factors, as well as the study of metabolic pathways based on ‘omics’ technologies, can play a very important role as a precise and effective approach in the fight against obesity (Morton et al., 2006; González-Muniesa et al., 2017; Kiseleva et al., 2024).

Being overweight is usually associated with a higher risk of developing chronic conditions such as type 2 diabetes, hypertension, atherosclerosis, dyslipidaemia, non-alcoholic steatohepatitis, reproductive problems, immune disorders, chronic low-grade inflammation and

certain types of cancer (Vasileva et al., 2018; Arner et al., 2019; Bluher, 2019; Wang et al., 2024). The etiological factors responsible for the development of obesity include: energy imbalance, genetic predisposition, neuroendocrine disorders, environmental and lifestyle factors, as well as certain drug therapies (Carayol et al., 2017; Bluher, 2019; Fathzadeh et al., 2020). In addition to being the primary energy store for fat, adipose tissue is an endocrine-active organ that determines the metabolic balance of the entire organism. Structurally, it consists of mature fat cells (adipocytes), their precursors – preadipocytes, stem cells, endothelial cells and various immune cells (Arner et al., 2019; Ramirez et al., 2020). In obese individuals, the expansion of adipose tissue is due to an increase in the size (hypertrophy) and/or number (hyperplasia) of fat cells, which contributes to increased infiltration by immune cells and the development of low-grade chronic inflammation and fibrosis (Horwitz and Birk 2023). Changes in adipose tissue during obesity lead to various types of stress – oxidative, metabolic and mechanical – which disrupt intra- and intercellular communication (Ramirez et al., 2020; Vasileva et al., 2020a; Wang et al., 2021; Zaghlool et al., 2021). Modulation of the adipogenic differentiation process is among the most widely used experimental approaches for managing obesity (Aprile et al., 2018; Mandl et al., 2019; Vasileva et al., 2021). Adipogenic differentiation is strictly regulated by the interaction between numerous transcription factors. The phosphoinositide 3-kinase (PI3K)/protein kinase B (AKT) pathway mediates cellular growth signals, such as that of insulin via the insulin receptor (INSR) on adipocytes, and thus influences the initiation of differentiation (Min et al., 2013; Ortega-Molina et al., 2015; Huang et al., 2018; Li et al., 2025). In the next stage, these signals are processed by key players such as CCAAT/enhancer-binding proteins (C/EBPs), peroxisome proliferator-activated receptors (PPARs) and sterol regulatory element-binding protein (SERBP). Together with the enzymes they regulate, which are responsible for lipid biosynthesis – such as fatty acid synthase (FASN) and acetyl-CoA carboxylase (ACC) – they contribute to the transformation of the precursor fat cell into a mature adipocyte (Vasileva et al., 2018; Mandl et al., 2019; Wang et al., 2021).

Approaches to managing obesity include restricting calorie intake, selecting specific nutrients – including the use of probiotics and prebiotics – regular physical exercise, and medication (orlistat, liraglutide, semaglutide, tirzepatide, phentermine in combination with topiramate), as well as surgical interventions (Ruban et al., 2019; Sannidhi et al., 2025).

Advances in scientific research into obesity highlight the need for a multi-component, individualised and long-term therapeutic approach to the treatment of this multifactorial condition, including psychological assessment, which may help to reduce anxiety (Baker et al., 2022). Furthermore, the molecular pathways of action of natural substances with the potential

to modulate the process of obesity are of particular importance. These compounds exert their effect through the following mechanisms: appetite suppression, inhibition of lipid absorption, alteration of adipocyte function, modulation of pancreatic β-cells and insulin sensitivity, and beneficial effects on the gut microbiota and obesity-associated chronic inflammation (Min et al., 2013; Vasileva et al., 2018; 2020b; 2021; Li et al., 2020a; Benbaibeche et al., 2025).

This doctoral thesis is based on an in-depth study of the effect of plant extracts from ethnopharmacologically used medicinal plants and their specific metabolites on the molecular mechanisms involved in the processes of lipogenesis and adipogenesis in human adipocytes. These studies are supplemented by experiments using a model organism – *Caenorhabditis elegans*. The model organism system used is cited as an appropriate approach for investigating the effect of biologically active substances on lipid metabolism and related diseases.

II. AIM AND OBJECTIVES

1. Objective

The aim of this thesis is to investigate the effects of extracts from the hairy lady's mantle (*A. monticola*) and the spiny restharrow (*O. spinosa*) and their secondary metabolites on adipogenesis and lipid accumulation in an *in vitro* model of human adipocytes, followed by *in vivo* validation of the most significant results in *C. elegans* nematodes.

2. Objectives

The following scientific tasks have been defined to achieve the main objective of this doctoral thesis:

2.1. Literature review on the traditional use of medicinal plants in metabolic disorders.

2.2. Phytochemical characterisation *via* NMR-based metabolic profiling of extracts from the selected plants.

2.3. *In silico* simulation of potential interactions between selected pure compounds from the extracts and target adipogenic protein structures.

2.4. Investigation of the anti-adipogenic potential of the selected extracts and their compounds in a human adipocyte obesity model.

2.5. Determination of the molecular mechanism of action of extracts from *Alchemilla* and *Ononis* and their bioactive compounds in an *in vitro* model of human adipocytes.

2.6. Validation of the anti-obesogenic potential of maackiain in an *in vivo* obesity model in *C. elegans*.

III. MATERIALS AND METHODS

1. Plant material and extraction

The collected plant material was freeze-dried using a VirTis BenchTop Pro apparatus with an Omnitronics™ controller from Genevac Ltd. (Ipswich, United Kingdom), followed by extraction in 50% methanol (1:30 w/v) using ultrasound for 20 minutes at room temperature. The extract was filtered, concentrated under vacuum at 40 °C, freeze-dried and stored at -20 °C until analysis.

2. Nuclear Magnetic Resonance spectroscopy profiling

The protocol for extraction, spectrum acquisition and subsequent analysis is described in detail by Georgiev et al. (2015). In brief, the spectral data from the proton (^{1}H) and 2D NMR analyses were acquired at 25 °C on a Bruker AVII+ 600 (Karlsruhe, Germany), operating at a frequency of 600.13 MHz with a relaxation time of 4.07 s. The processing and analysis of the spectral data was carried out using the specialised software MestreNova (Mestrelab Research, Santiago de Compostela, Spain).

3. Molecular docking analysis

Docking calculations were performed using Autodock Vina software on PyRx 0.8. The crystal structures of the target proteins were obtained from the Protein Data Bank (PDB, www.wwpdb.org) with the following PDB IDs: 1NWQ for C/EBPα; 2P4Y for PPARγ, 1O6L for AKT, 5ITD for PI3K. To prepare the proteins for docking simulation, all water molecules and co-crystallised heteromolecules were removed, followed by the addition of hydrogen atoms and neutralisation using Coleman's unified atomic charges.

4. Cell culture and treatment

Human SGBS preadipocytes were cultured and differentiated in accordance with optimal conditions (Vasileva et al., 2020b; Wabitsch et al., 2001). In parallel with the induction of adipogenic differentiation (day 0), the cells were treated upon medium change on days 4 and^8, respectively. All concentrations used were selected following an assessment of cell viability via MTT assay. Extracts from the aerial parts of *A. monticola* (ALM) and roots of *O. spinosa* (OSR) were added to the culture medium at final concentrations of 5, 10 and 25 μg/mL, whilst the pure compounds AST, QUE, ONON were applied at concentrations of 5, 10, 25 μM, and MACK at concentrations of 5, 10, 25 and 50 μM. The control group was treated with 0.2%

DMSO as a vehicle. All analyses were performed 24 hours after the final treatment, i.e. on the 9th day of differentiation, in at least three independent biological experiments.

5. Analysis of intracellular lipid accumulation and free glycerol release

Following fixation with formalin, differentiated SGBS adipocytes were stained with an ORO solution, as described previously (Vasileva et al., 2020b). Quantification of accumulated lipids was performed by measuring the absorbance of the ORO stain at 495 nm on an Anthos Zenyth 340 spectrophotometer from Biochrom Ltd. (Cambridge, United Kingdom), extracted from the adipocytes after staining.

The free glycerol content in the culture medium was measured using an adipolysis assay kit (cat. no. MAK313) from Merck KGaA, in accordance with the manufacturer's instructions.

6. Quantitative real-time polymerase chain reaction (RT-qPCR)

Total RNA was isolated using the Quick-RNA Miniprep Kit from Zymo Research (Ivrine, CA, USA). Reverse transcription was performed using the Canvax FirstStrand cDNA Kit (Cordoba, Spain). The expression of key adipogenic genes was assessed using the RT-qPCR , utilising Sso EvaGreen SuperMix on a CFX96 system (Bio-Rad). Relative gene expression was determined using the comparative threshold cycle method ($_{\Delta\Delta}C_T$) in the CFX Maestro software (Bio-Rad) relative to ribosomal protein L13a (RPL13A) and beta-tubulin (TUBB) as reference genes.

7. Protein detection by immunoblot analysis

Total protein lysates were prepared and analysed by Western blotting, as described previously (Vasileva et al., 2021). Equivalent amounts of 30 μg protein samples were separated by sodium dodecyl sulphate-polyacrylamide gel electrophoresis and transferred to nitrocellulose membranes. Protein data were normalised against a reference protein using Image Lab 6.0.1 software (Bio-Rad).

8. Model of glucose-induced lipid accumulation in *C. elegans*

Wild-type N2 Bristol *C. elegans* nematodes and *Escherichia coli* OP50 (*E. coli* OP50) were purchased from the Caenorhabditis Genetic Centre (CGC, University of Minnesota). The nematodes were cultured under conditions in accordance with the manufacturer's protocol. An age-synchronised population was obtained by treating adult individuals in the reproductive phase with a sodium hypochlorite solution. During the first two larval stages (approximately

24 hours), the nematodes were cultured on Petri dishes containing NGM medium with or without 2% glucose. In the next stage, the nematodes were transferred to fresh Petri dishes containing NGM, pre-treated with MACK (25, 50 and 100 μM) or 0.1% DMSO as a vehicle added to the food source. Orlistat (ORST) at a concentration of 12 μM was used as the anti-obesogenic (positive control. The doses used for treatment with MACK were selected based on viability analysis.

The *E. coli* OP50 bacterial culture used was heat-inactivated to prevent the possibility of ORST and MACK being metabolised by the bacteria themselves. Fourth-stage (L4) nematodes collected by washing with M9 buffer were subjected to the following analyses: staining of lipid accumulations and confocal microscopy, as well as total RNA isolation.

9. Nematode viability assay

The extent to which nematode viability was affected 48 hours after treatment was assessed using the 3-(4,5-dimethylthiazol-2-yl)-2,5-diphenyl tetrazolium bromide (MTT) assay, described in detail in Savova et al. (2022).

To confirm that the pure active substance MACK has no effect on nematode viability, an MTT test was performed. Synchronised L4-stage nematodes were treated with MACK at concentrations ranging from 10 to 200 μg/mL.

10. Assessment of locomotor activity in *C. elegans*

The number of nematode bends over a 30-second period was recorded, as described in Savova et al. (2022). Following treatment with the selected experimental concentrations of MACK, the larvae were transferred to NGM without *E. coli* OP50 to acclimatise. The number of nematode bends in a drop (5 μL) of M9 buffer was recorded over a 30-second period, with 15 nematodes per group used for the analysis.

11. Chemotaxis in response to experimental treatment in *C. elegans*

Caenorhabditis elegans utilises its highly developed chemosensory system, comprising amphidial, phasmidial and internal labial neurons, in food foraging, mate finding, egg laying, as well as for avoiding pathogens and toxic substances (Queiros et al., 2021). Thus, in the context of treatment with natural molecules, chemotaxis analysis provides information on both the neurobiological state of the model organism and the behavioural attraction/aversion responses, as well as the ability to track the nematode's affinity for a given substance.

12. Staining of lipid droplets in nematodes

Nile red (NR) is used as a stain. The staining of lipid accumulations and their subsequent quantification in *C. elegans* is performed according to the protocol cited in Savova et al. (2022). Representative images are analysed using software (ImageJ), and the fluorescent signal is converted to corrected total cell fluorescence (CTCF).

13. Quantitative real-time polymerase chain reaction (RT-qPCR) for the analysis of RNA and microRNA in an in vivo model of *C. elegans*

Groups of approximately 3,000-4,000 nematodes treated respectively with MACK (100 μM), orlistat (12 μM), a combination of MACK (100 μM) and orlistat (12 μM), and a control group (vehicle; with a final concentration of 0.4% DMSO) were used to isolate RNA using PureZol (Bio-Rad), in accordance with the manufacturer's protocol. CFX Maestro 1.1 software (Bio-Rad) was used for quantitative analysis of RNA expression using the $_{\Delta\Delta}$CT method. The iscu-1 and mdh-1 RNAs were used as endogenous controls, and the results were normalised against the vehicle-treated group. Reverse transcription of microRNAs was performed using steam-loop primers and the Revert Aid H Minus First Strand cDNA synthesis kit from Thermo Fisher Scientific (Waltham, MA, USA). Quantitative analysis of miRNA expression was performed using the CFX Maestro 1.1 software (Bio-Rad) via the ΔΔCT method. Reference miRNAs were used, namely the exogenous control ath-miR-159a and the endogenous U18.

14. Determination of protein levels by Western blot analysis in an in *vivo C. elegans* model

Total protein lysates from nematodes were prepared using ice-cold RIPA buffer and quantified using the Bradford assay. Equal volumes of the protein lysates were subjected to electrophoresis on a 10% sodium dodecyl sulphate-polyacrylamide gel and transferred to a nitrocellulose membrane blocked for 1 hour at room temperature in 5% (w/v) skimmed milk in Tris-buffered saline. Overnight incubation was performed with the primary anti-pAMPK antibody, followed by a 1-hour incubation with SB700-conjugated secondary antibody. Visualisation was performed using a ChemiDoc MP system (Bio-Rad). The amount of target protein was normalised against β-actin using Image Lab 6.0.1 software (Bio-Rad).

15. Statistical analysis

The data obtained were analysed using SigmaPlot v11.0 software from Systat Software GmbH (Erkrath, Germany) and presented as mean ± standard error of the mean (SEM). Differences

between groups were determined using Student's t-test where appropriate, or one-way analysis of variance (ANOVA), followed by Bonferroni *post hoc* analysis when comparing more than two groups. Values of *$p < 0.05$ and **$p < 0.001$ were considered statistically significant.

IV. RESULTS

1. Metabolic profiling of the experimental extracts

1.1. Extract from the aerial parts of *A. monticola*

The phytochemical characterisation of the ALM extract was carried out using NMR-based metabolic profiling (Figure 1). According to the analysis of the proton (^{1} H) NMR spectrum, the most abundant signals correspond to organic acids and flavonoids – astragalin, catechin, quercetin, quercetin-3-O-β-glucuronide, quercitrin, isoquercetin, rutin, vanillic acid and vitexin (Table 1).

Table 1. Identified metabolites in *A. monticola* extract. The chemical shift (δ) and coupling constant (J) of the metabolites in the extract were determined by comparing the obtained NMR spectra with literature data (Chang et al., 2009; Kuruüzüm-uz et al., 2013; Wolfender et al., 2013; Ganbaatar et al., 2016; Mandrone et al., 2018)

Metabolite	**Chemical shift (δ, ppm)**	**Multiplicity/coupling constant (J, Hz)**
Amino acids		
Alanine	1.48	(d, J = 7.4)
Threonine	1.33	(d, J = 6.5)
Valine	1.00/1.02	(d, J = 7.2)/(d, J = 7.0)
Sugars		
α-Glucose	5.18	(d, J = 3.7)
β-Glucose	4.58	(d, J = 7.8)
Sucrose	5.40/4.17	(d, J = 3.6)/(d, J = 8.7)
Fructose	3.62/3.69/4.03	(m)/(m)/(m)
Organic acids		
Fumaric acid	8.45	(s)
Succinic acid	2.52	(s)
Phenolic acids		
Vanillic acid	7.58/7.55/6.87/3.93	(d, J = 2.0)/(dd, J = 8.5; 2.2)/(d, J = 8.2)/(s)
Flavonoids and flavonoid glucosides		
Astragalin	6.28/6.48/6.97/8.04/5.23	(d, J = 2.0)/(d, J = 2.0)/(d, J = 8.5)/(d, J = 8.6)/(d, J = 7.8)
Catechin	4.69/4.14/2.82/2.49/6.02/6.03/6.88/ 6.87/6.79	(d, J = 7.4)/(td, J = 8.1; 4.3)/(dd, J = 16.5; 8.3)/(dd, J = 16.0; 8.7)/(d, J =

		2.0)/(d, *J* = 2.0)/(d, *J* = 2.0)/(d, *J* = 8.2)/(dd, *J* = 8.4; 2.3)
Isoquercitrin	6.28/6.48/7.68/6.97/7.55/5.23	(d, *J* = 2.0)/(d, *J* = 2.0)/(d, *J* = 2.0)/(d, *J* = 8.5)/(dd, *J* = 8.5; 2.2)/(d, *J* = 7.8)
Kaempferol	6.28/6.48/7.00/8.04	(d, *J* = 2.0)/(d, *J* = 2.0)/(d, *J* = 8.5)/(d, *J* = 8.6)
Quercetin	6.28/6.48/7.72/6.97/7.64	(d, *J* = 2.0)/(d, *J* = 2.0)/(d, *J* = 2.0)/(d, *J* = 8.5)/(dd, *J* = 8.5; 2.3)
Quercetin-3-*O*-β-glucuronide	7.73/7.55/6.87/6.42/6.28/5.23	(d, *J* = 2.0)/(dd, *J* = 8.5; 2.2)/(d, *J* = 8.2)/(d, *J* = 2.2)/(d, *J* = 2.2)/(d, *J* = 7.8)
Quercitrin	6.28/6.42/7.31/7.00/7.55/5.270.97	(d, *J* = 1.8)/(s)/(d, *J* = 2.0)/(d, *J* = 8.5)/(dd, *J* = 8.4; 2.0)/(d, *J* = 1.6)/(d, *J* = 6.3)
Rutin	6.28/6.48/7.68/6.97/7.64/5.06/4.54	(d, *J* = 2.0)/(d, *J* = 2.0)/(d, *J* = 2.0)/(d, *J* = 8.5)/(dd, *J* = 8.8; 2.4)/(d, *J* = 8.2-Glu)/(d, *J* = 2.0-Rha)
Vitexin	6.69/6.37/8.00/7.92/7.00/5.10	(s)/(s)/(d, *J* = 8.9)/(s)/(d, *J* = 8.5)/(d, *J* = 10.1)
Others		
Inositol	3.91/3.61/3.20	(m)/(m)/(m)
γ-Aminobutyrate	1.90/2.32/3/01	(m)/(t, *J* = 7.5)/(t, *J* = 7.5)

The structures of some of the molecules, such as AST and QUE, were observed in both ^{1}H NMR and heteronuclear single-quantum coherence (HSQC) spectroscopy. With regard to astragalin, several signals typical of aromatic hydrogens were observed in the two-dimensional HSQC spectrum of the ALM extract: two doublets at δ_H 6.28 and δ_H 6.46, which correlate with the carbon resonance at δ_C 101.66 and δ_C 97.02 and corresponds to the meta-bonding of H6 and H8 protons, corresponding to the flavonoid A-ring. Two other doublets with ortho-bonding constants at δ_H 6.97 and δ_H 8.04 are correlated with δ_C 118.36 and δ_C 131.33 and correspond to H3′/5′ and H2′/6′, suggesting two para-substituted flavonoid B-rings. The anomeric proton (H1″) of glucose appears at δ_H 5.*23*/δ_C 105.12. Compared with previously published data (Rezende et al., 2019), the structure can be considered to correspond to astragalin.

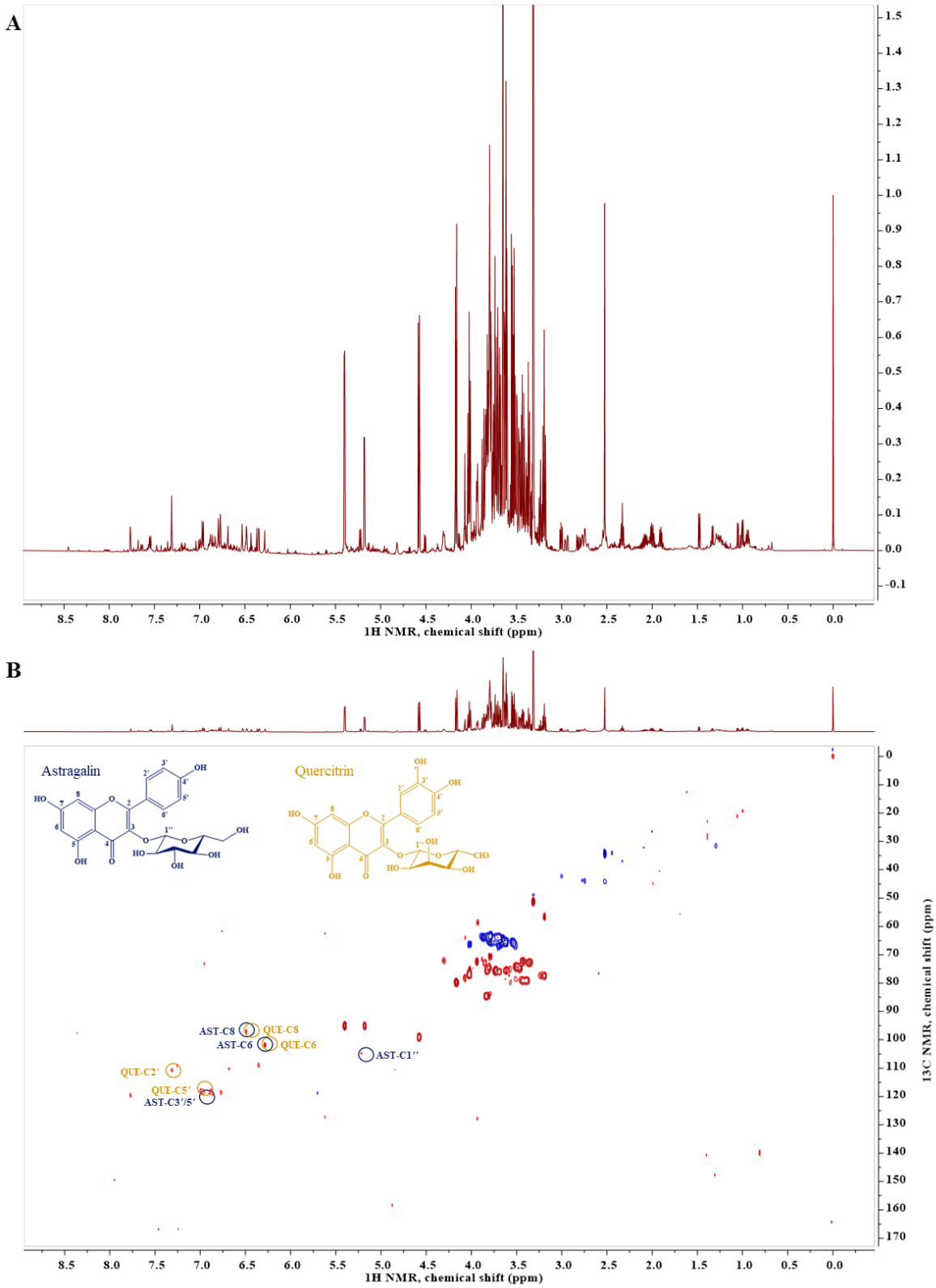

Figure 1. Representative NMR spectra of an extract from *Alchemilla monticola*. Proton ^{1} H NMR (600 MHz) spectrum (A) and data from heteronuclear single-quantum coherent spectroscopy (^{1}H-^{13}C HSQC) with the characteristic signals of astragalin (AST) and quercitrin (QUE) highlighted (B).

In quercitrin, the intersection of the δ_H 5.*27*/δ_C 93.36 signals suggests the presence of an α-linked rhamnose moiety. The protons in the A-ring (H6 and H8) of the flavonoid nucleus have been identified based on the HSQC correlations δ_H 6.*28*/δ_C 101.66 and δ_H 6.*42*/δ_C 97.02. The correlation between signals at δ_H 7.*31*/δ_C 110.98, δ_H 7.*00*/δ_C 117.98 and δ_H 7.*5*/δ_C 125.02 correspond to protons H2′, H5′ and *H6′* of the B-ring, suggesting a quercitrin core (Wolfender et al., 2013).

Based on the results of the metabolic profiling of ALM, AST and QUE were selected for further *in silico* assessment of anti-adipogenic potential.

1.2. *Ononis spinosa* root extract

Metabolic profiling of OSR was also performed by analysing one- and two-dimensional NMR spectra. In the proton spectrum, the most abundant signals correspond to ononin, sativanone, onogenin and maackiain (Figure 2 and Table 2).

Table 2. Identified metabolites in O. spinosa extract. Chemical shifts (δ) and coupling constants (J) of the identified metabolites based on their respective 1H NMR spectra (Bernhardt et al., 2000; Park et al., 2003 and Wu et al., 2020).

Metabolite	**Chemical shift (ppm)**	**Multiplicity/coupling constant (Hz)**
Amino acids		
Alanine	1.48	(d, *J* = 7.3)
Glutamine	2.13/2.46	(m)/(m)
Valine	1.00	(d, *J* = 7.0)
Leucine	0.96	(d, J = 7.0)
Sugars		
β-Glucose	4.58	(d, *J* = 7.9)
Sucrose	5.40/4.17	(d, *J* = 3.8)/ (d, *J* = 8.6)
Organic acids		
Acetic acid	1.96	(s)
Fumaric acid	6.54	(s)
Malic acid	2.82/2.95	(dd, *J* = 16.9, 8.4)/(dd, *J* = 16.9, 4.0)
Flavonoids and flavonoid glucosides		

Ononin	6.02/7.38/6.55/6.84/6.96/6.82/5.01/ 3.60	(s)/(d, *J* = 8.7)/(dd, *J* = 8.3, 2.3)/(d, *J* = 2.50)/(dd, *J* = 8.0, 2.7)/(dd, *J* = 8.6, 2.5)/(d, *J* = 7.6)/(s)
Sativanone	4.45-4.51/4.30/4.34/4.23/7.86/6.55/ 6.29/3.71/3.78/6.56/7.06	(m)/(m)/(dd, *J* = 12.2, 5.6)/(d, *J* = 8.9)/(dd, *J* = 8.3, 2.3)/(d, *J* = 2.3)/(s)/(s)/(d, *J* = 2.3)/(d, *J* = 8.9)
Onogenin	4.45-4.51/4.30-4.34/4.23/7.86/6.55/ 6.29/3.71/6.69/6.61	(m)/(m)/(dd, *J* = 12.2, 5.6)/(d, *J* = 8.9)/(dd, *J* = 8.3, 2.3)/(d, *J* = 2.3)/(d, *J* = 1.0)/(s)/(s)/(s)
Spinonin	6.13/6.12/6.84/6.55/7.38/3.23/2.74/ 6.89/5.01	(m)/(d, *J* = 1.2)/(d, *J* = 2.5)/(dd, *J* = 8.3, 2.3)/(d, *J* = 8.7)/(dd, *J* = 14.1, 7.1)/(dd, *J* = 16.0, 4.2)/(d, *J* = 8.6)/(d, *J* = 7.5)
Maackiain	7.27/6.55/6.29/3.55/3.23/4.23/6.26/ 6.42/5.60/5.90	(d, *J* =8.4)/(dd, *J* = 8.3,2.3) / (d, *J* =2.5)/(t, *J* =10.6)/(m)/ (m)/(s)/(s)/(d, *J* = 7.4)/(dd, *J* = 15.5, 1.0)
Others		
Formic acid	8.46	(s)
γ- Aminobutyric acid	1.9/2.32/3.01	(m)/(t, *J* = 7.2)/(t, *J* = 7.3)
Choline	3.21 (s)	3.21 (s)

The structure of ononin was identified via its ^{1}H NMR and HSQC spectra (Figure 7A). In the ^{1}H NMR spectrum, the three protons H-5, H-6 and H-8 of ring A represent an ABX spin system. The H-5 signal shows a coupling constant *J* = 8.7 Hz (δ_H 7.*3*/δ_C 131.26), which confirms the ortho coupling to H-6 *J* = 8.3; 2.3 Hz (δ_H 6.*55*/δ_C 114.87). The signal of H-6 indicates not only an ortho- but also a meta-bond to H-8 with *J* = 2.5 Hz (δ_H 6.*84*/δ_C 110.37). The two signals at δ_H 6.96 δ_C 114.92 *(J* = 8.0; 2.7) and δ_H 6.*82*/δ_C 110.74 (*J* = 8.6; 2.5) characterise the B-ring system of the aromatic protons H-2′/H-6′ and H-3′/H-5′. The signals of the –OCH_3 group were detected at δ_H 3.60/δ_C 63.38 (s). The coupling constants of the anomeric proton signal H-1′, *J* = 7.3 Hz (δ_H 5.*01*/δ_C 99.81) confirm the presence of β-glucopyranose (Bernhardt et al., 2000).

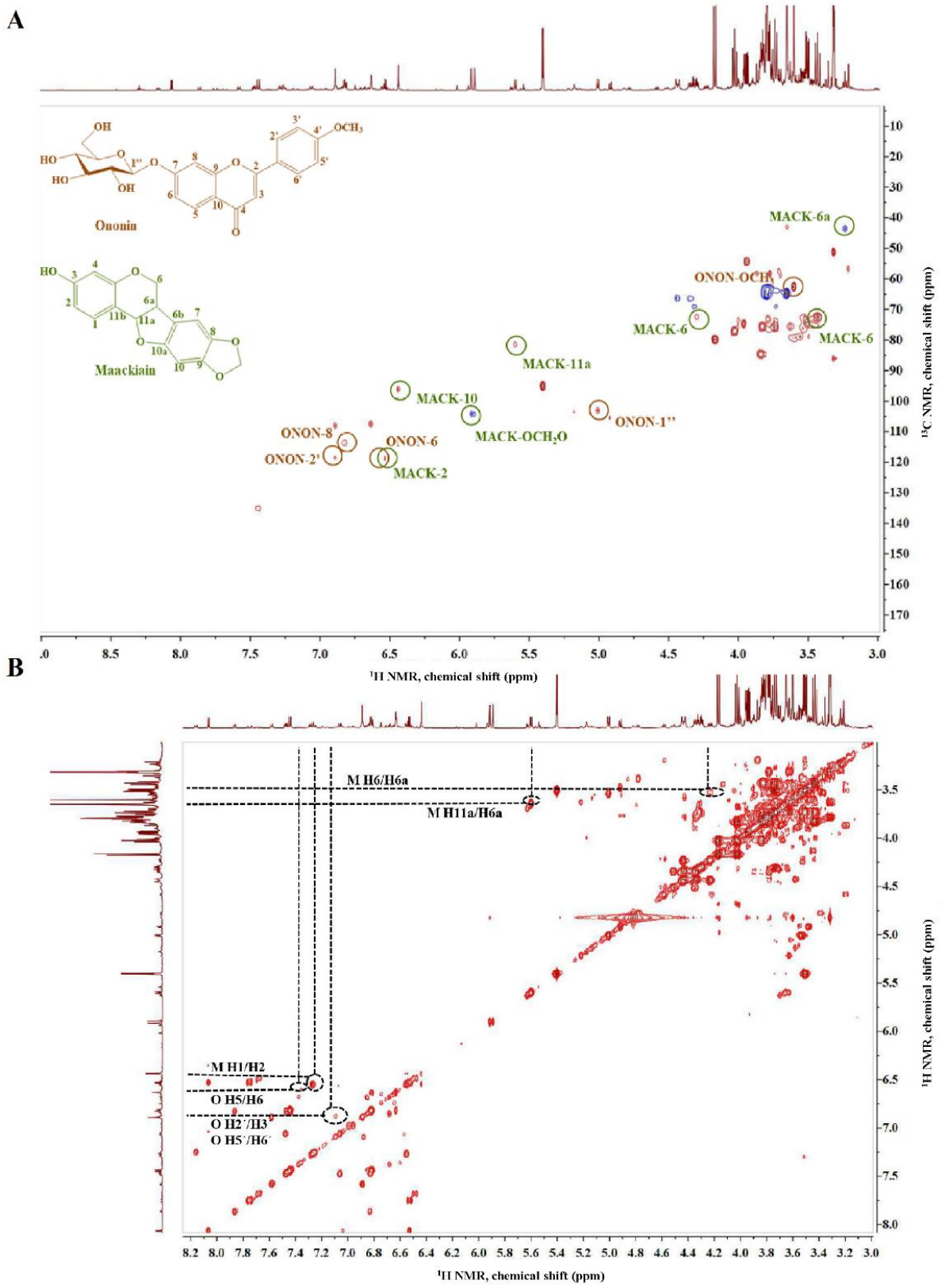

Figure 2. Spectra from heteronuclear single-quantum coherent spectroscopy (^{1}H-^{13}C HSQC, A) and ^{1}H–^{1}H homonuclear correlation spectroscopy (^{1}H–^{1}H COSY, B) spectra of *an O. spinosa* extract and characteristic signals of ononin (O) and maackiain (M).

The presence of maackiain was confirmed by a set of peaks corresponding to the pterocarpane skeleton, i.e. signals such as δ_H 5.*60*/δ_C 80.50 (d, *J* = 7.4 Hz), δ_H 4.*2*/δ_C 72.89 (m), δ_H 3.*55*/δ_C 72.89 (t , *J* = 10.7) and δ_H 3.*23*/δ_C 43.23 (m) are assigned to H-11a, H-6, H-6 and H-6a, respectively. A doublet at δ_H 5.*90*/δ_C 104.31 (*J* = 5.5; 1.0 Hz), corresponding to -OCH_2 O-, and a singlet each at δ_H 6.*42*/δ_C 96.22 (s) and δ_H 7.*26*/δ_C 113.25, corresponding to H-10 and H-8, respectively, suggesting a methylenedioxy moiety in the aromatic D ring. Furthermore, a doublet at δ_H 6.*29*/δ_C 104.5 (*J* = 2.5 Hz; H-4), a doublet at δ_H 6.*5*/δ_C 111.4 (*J* = 8.4; 2.3 Hz) and a doublet at δ_H 7.*27*/δ_C 124.56 *(J* = 8.4; H-1), assigned to the ABX system of the A ring (Park et al., 2003; Wu et al., 2020).

Based on metabolic profiling, OSR, ONON and MACK were selected for further *in silico* evaluation of anti-adipogenic potential.

2. *In silico* docking simulation

The affinity of the selected pure substances for the proteins is expressed in terms of the free energy of binding ($_{\Delta}G$) and the binding constant ($_{K\_i}$; Table 3 for AST and QUE, and Table 4 for MACK and ONON). All calculated affinity constants for AST are in the range 0.2–24.4 μM, for QUE 0.4–24.4 μM, for ONON 0.06–14.7 μM and for MACK 0.4– 67.2 μM. The lowest binding free energy values for AST and QUE are observed with PI3K and PPARγ, and for ONON and MACK with AMPK, PI3K and PPARγ. Their orientation and binding sites on the target proteins are shown in Figure 8 for AST and QUE, and in Figures 3 and 4 for ONON and MACK.

Table 3. Free binding energy ($_{\Delta}G$, kcal/M) and affinity constant (K_i, μM) for QUE and AST to the target protein structure.

Target protein	Quercitrin	Astragalin
C/EBPα (PDB: 1NWQ)	-6.3 kcal/M; 24.4 μM	-6.3 kcal/M; 24.4 μM
PPARγ (PDB: 2P4Y)	-7.8 kcal/M; 1.9 μM	-7.3 kcal/M; 4.5 μM
AKT (PDB: 1O6L)	-6.8 kcal/M; 10.5 μM	-6.7 kcal/M; 12.4 μM
PI3K (PDB: 5ITD)	-8.7 kcal/M; 0.4 μM	-9.2 kcal/M; 0.2 μM

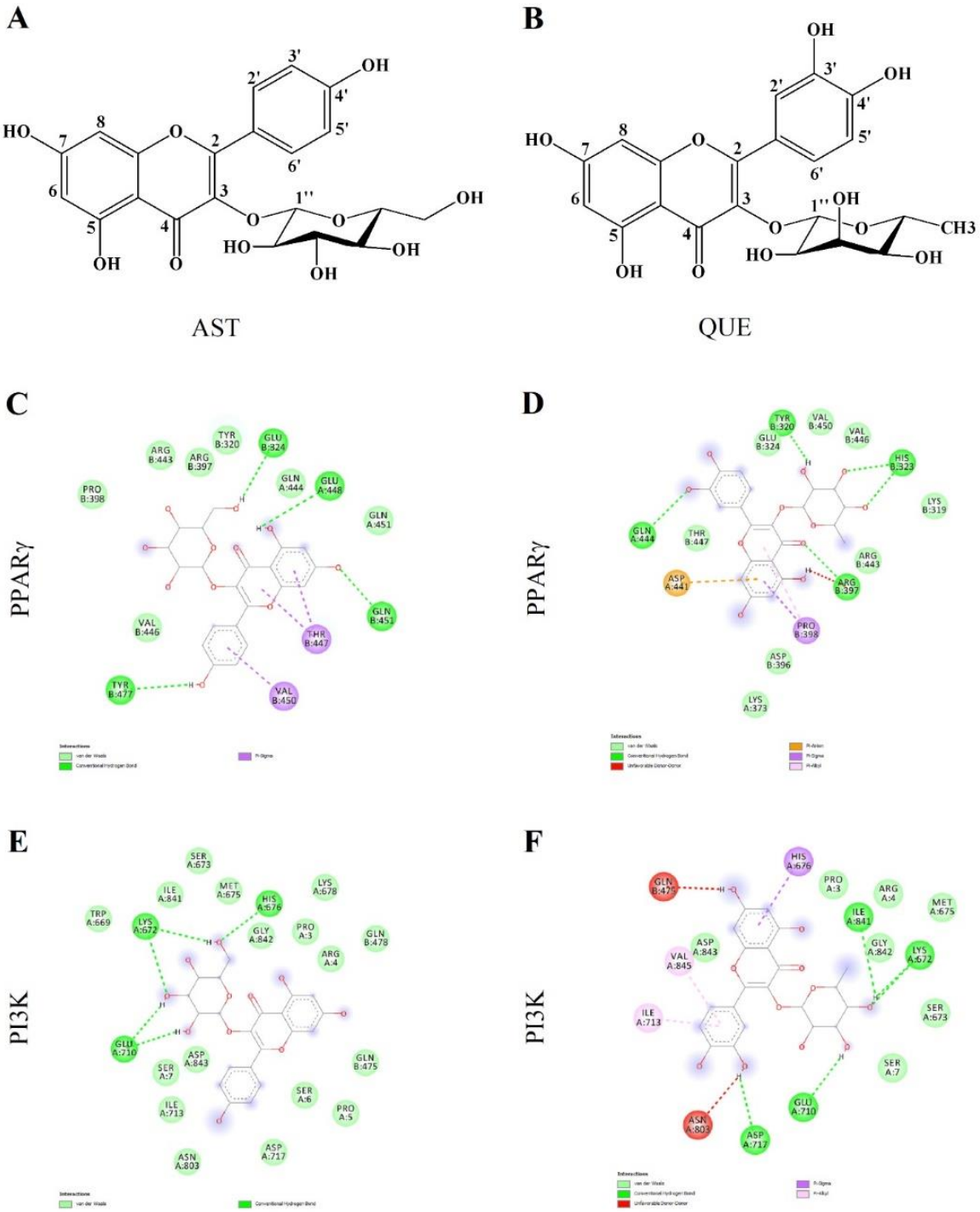

Figure 3. Astragalin (AST) and quercitrin (QUE) exhibit strong affinity for the protein structures of PPARγ and PI3K. Chemical name of AST: 5,7-dihydroxy-2-(4-hydroxyphenyl)-3-[(2S, 3R, 4S, 5S, 6R)-3,4,5-trihydroxy-6-(hydroxymethyl)-oxan-2-yl]-oxychromen-4-one (A) and for QUE: 2-(3,4-dihydroxyphenyl)-5,7-dihydroxy-3-[(2S, 3R, 4R, 5R, 6S)-3,4,5-trihydroxy-6-methyloxan-2-yl]-oxochromene-4-one (B). Potential molecular interactions between AST and PPARγ (C); QUE and PPARγ (D); AST and PI3K (E); QUE and PI3K (F).

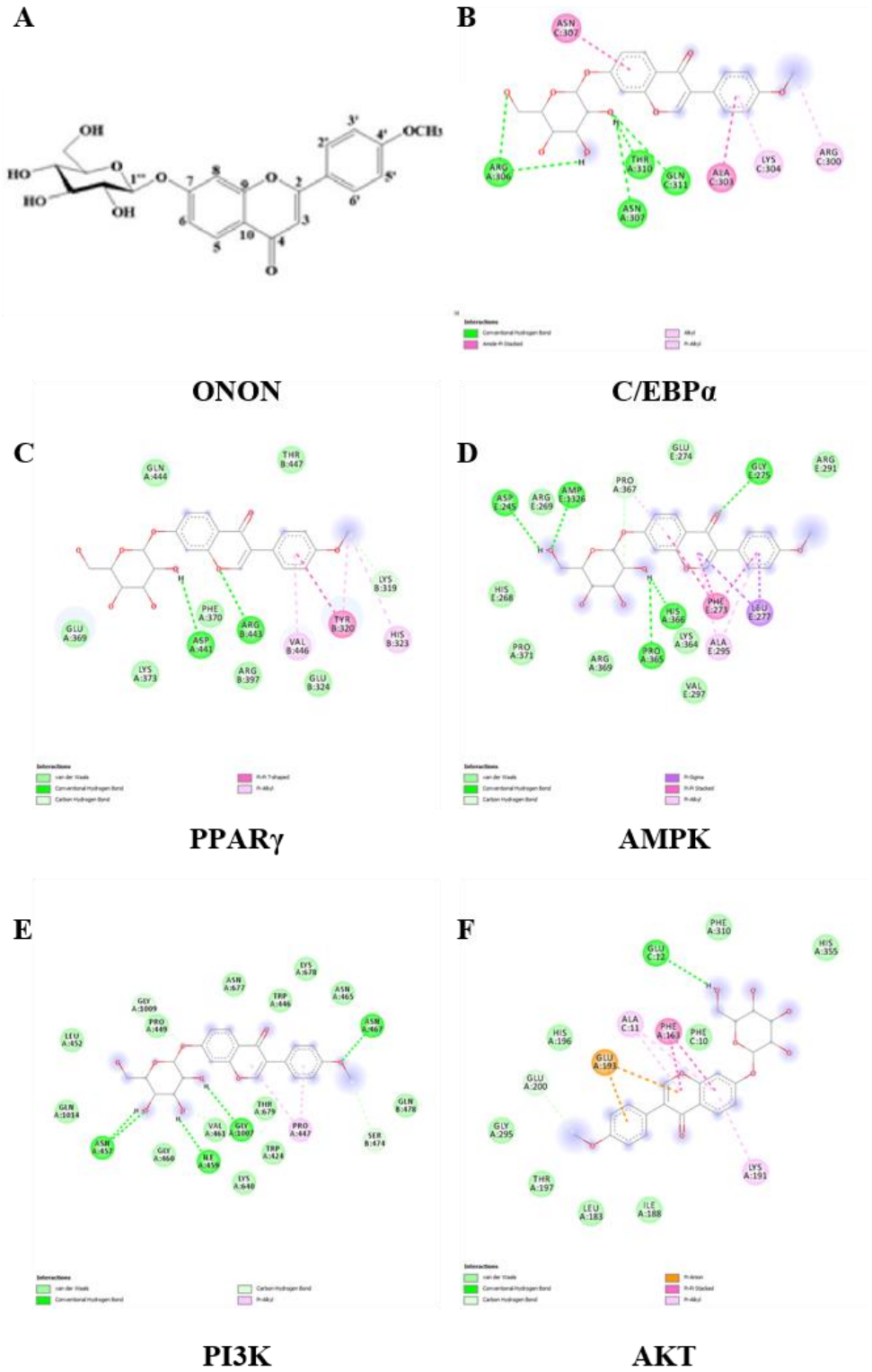

Figure 4. Based on the calculations performed, ononin (ONON) binds with the highest affinity to the protein structures of PPARγ, PI3K, AMPK and AKT. Chemical name of ONON: 3-(4-methoxyphenyl)-7-[(2S,3R,4S,5S,6R)-3,4,5-trihydroxy-6-(hydroxymethyl)oxan-2-yl]oxychromen-4-one (A). Potential interactions between: ONON and CEBPα (B); ONON and PPARγ (C); ONON and AMPK (D); ONON and PI3K (E); ONON and AKT (F).

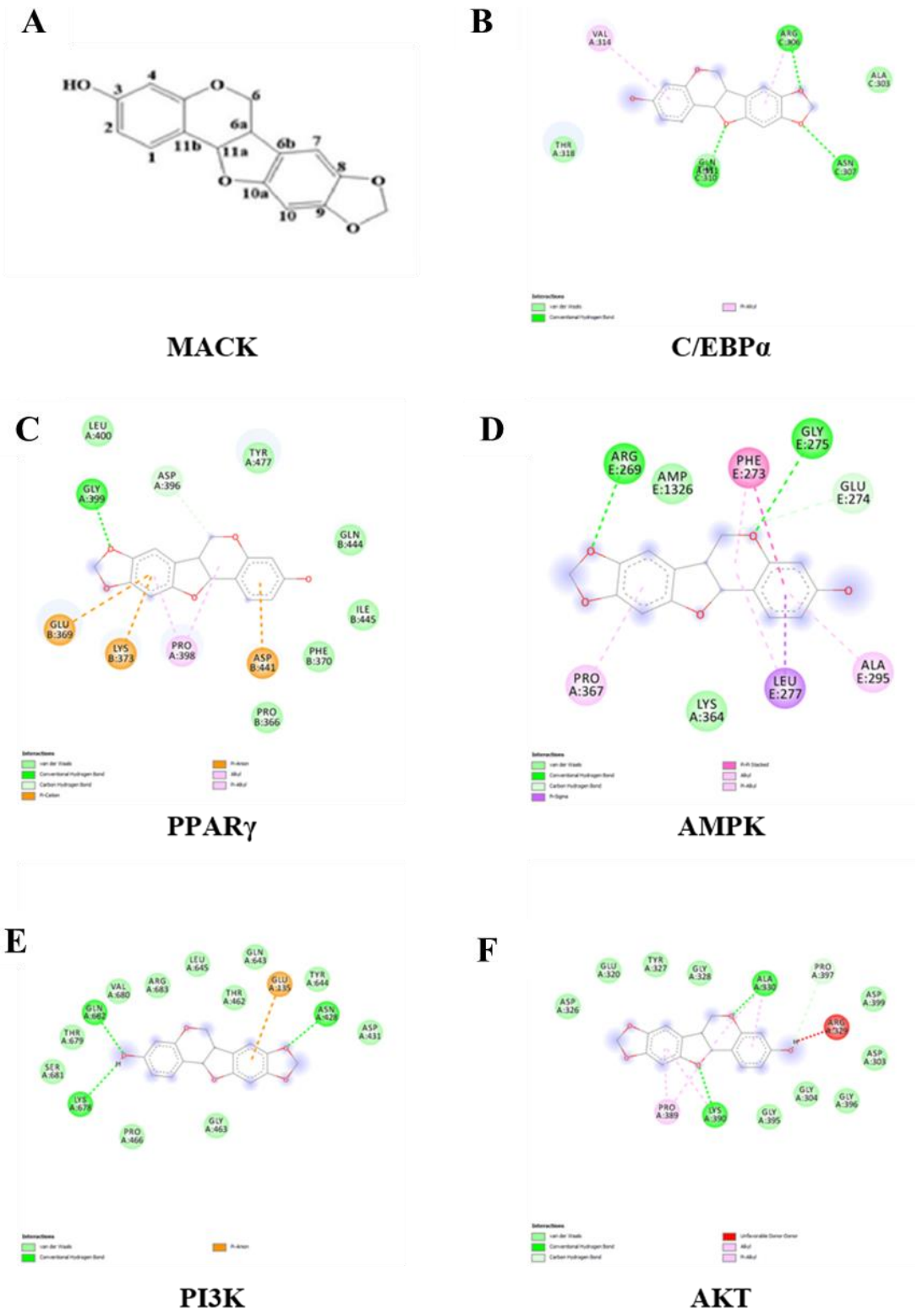

Figure 5. Theoretically, maackiain (MACK) binds with the highest affinity to PPARγ, PI3K, AMPK and AKT. Chemical name of MACK: (1R,12R)-5,7,11,19-tetraoxapentacyclo-[10.8.0.$0^{2,10}$.$0^{4,8}$.$0^{13,18}$]icosa-2,4(8),9,13(18),14, 16-hexen-16-ol (A). Potential interactions between: MACK and CEBPα (B); MACK and PPARγ (C); MACK and AMPK (D); MACK and PI3K (E); MACK and AKT (F).

Table 4. Binding free energy ($_{\Delta}G$, kcal/M) and affinity constant (K_i, μM) for ONON and MACK to the structure of the respective target protein

Target protein	Ononin	Maackiain
C/EBPα (PDB: 1NWQ)	-6.6 kcal/M; 14.7 μM	-5.7 kcal/M; 67.2 μM
PPARγ рецептор (PDB: 2P4Y)	-7.9 kcal/M; 1.6 μM	-7.9 kcal/M; 1.6 μM
AMPK (PDB: 4CFF)	-9.9 kcal/M; 0.06μM	-8.8 kcal/M; 0.4 μM
AKT (PDB: 1O6L)	-7.4 kcal/M; 3.8 μM	-7.8 kcal/Ml; 1.9 μM
PI3K (PDB: 5ITD)	-9.0 kcal/M; 0.3 μM	-8.6 kcal/M; 0.5 μM

3. Evaluation of the anti-adipogenic potential of *A. monticola* extract, astragalin (AST) and quercetin (QUE) in an *in vitro* model of human adipocytes

3.1. Adipogenesis and lipolysis following treatment with *A. monticola* extract and selected pure compounds

Lipid accumulation is reduced in the model system of human adipocytes treated with *A. monticola* extract. Assessment of lipid accumulation by ORO analysis indicates significant anti-adipogenic activity of ALM (Figure 6).

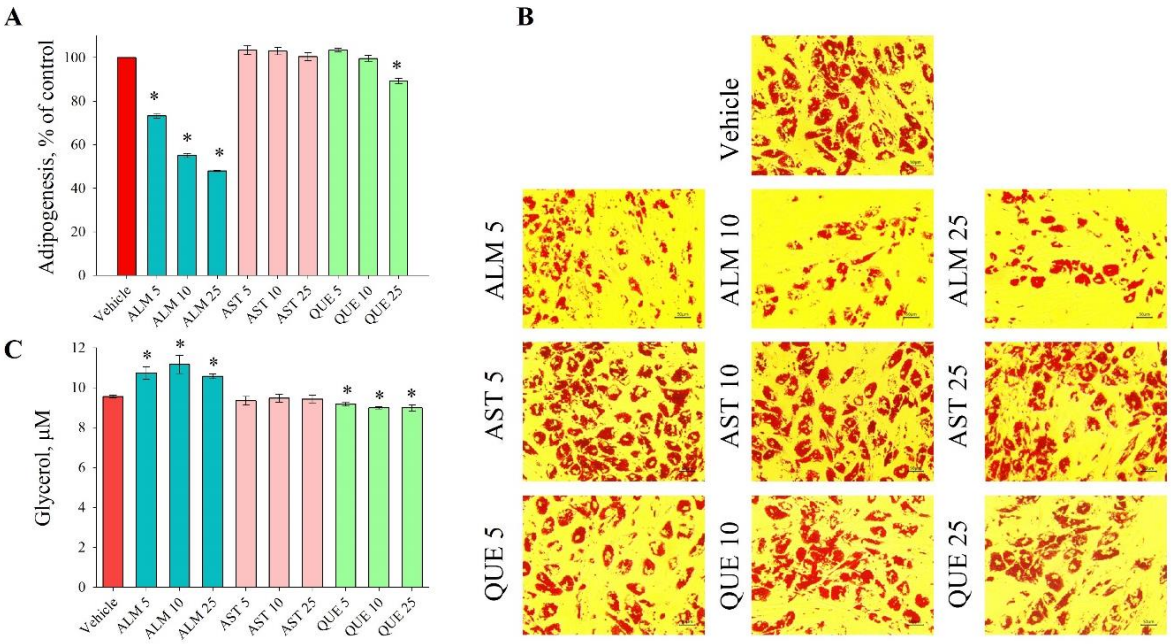

Figure 6. *A. monticola* extract (ALM) reduces lipid accumulation in human adipocytes. Lipid content, expressed as a percentage of the control group (Vehicle), in adipocytes treated with ALM 5, 10 and 25 μg/mL, astragalin (AST) 5, 10 and 25 μM, and quercitrin (QUE) 5, 10 and 25 μM from the ORO assay (A). Representative images (magnification ×20) of all experimental

groups following ORO staining (B). Assessment of free glycerol in the culture medium on day 9 of differentiation (C). Data are expressed as mean ± SEM, *p < 0.05 compared to the vehicle group (Vehicle, 0.2% DMSO).

The results indicate that treatment with ALM extract enhances basal lipolysis , as evidenced by the increased amount of free glycerol in the culture medium (Figure 6C). In this experiment, neither adipogenesis nor lipolysis processes were affected by treatment with AST (Figure 6A, 6C). With regard to the effect of QUE, a significant reduction in accumulated lipids was observed only at the highest concentration used (Figure 6A, 6B), whilst lipolysis levels were moderately reduced (Figure 6C) at all three concentrations applied. These data suggest that the ALM extract possesses anti-adipogenic potential, which may be partially dependent on the presence of AST and QUE in the extract.

3.2. Analysis of gene expression by RT-qPCR of *A. monticola* extract and pure compounds

To identify the main molecular pathways of adipogenesis influenced by ALM and its secondary metabolites, the expression levels of messenger RNA for key adipogenic factors and genes involved in lipid biosynthesis were assessed using RT-qPCR (Figure 7).

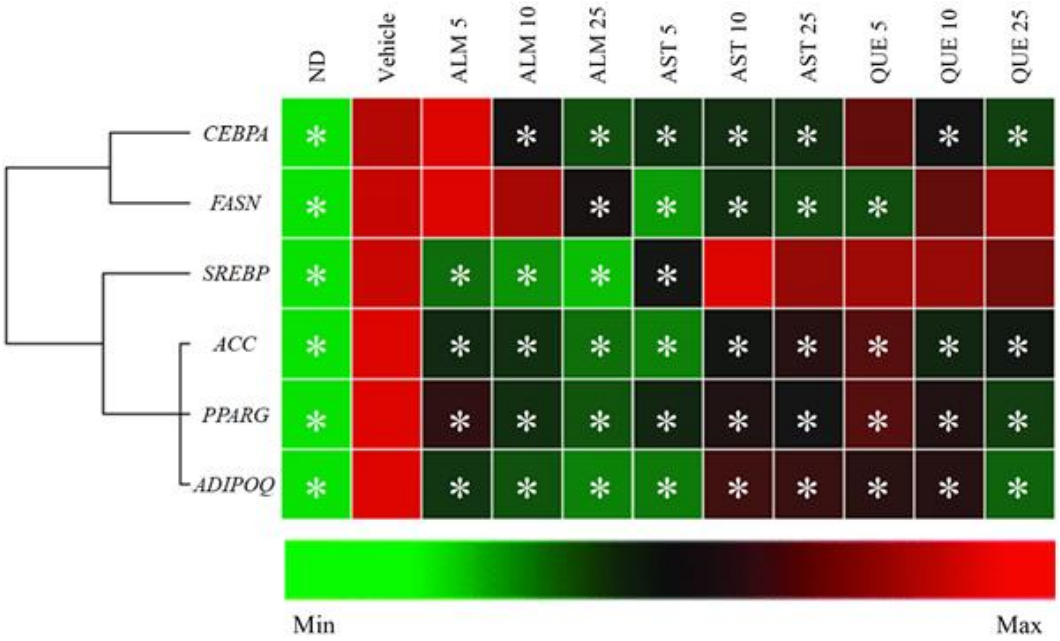

Figure 7. Analysis of adipocyte differentiation genes following treatment with *A. monticola* extract (ALM), astragalin (AST) and quercitrin (QUE). Relative mRNA expression, normalised to the vehicle control group, ($_{\Delta\Delta}$Cq) for *ACC, ADIPOQ, CEBPA, FASN, PPARG*

and *SREBP-1* from the RT-qPCR analysis. Data are presented as mean ± SEM. * $p < 0.05$ compared to the vehicle group – 0.2% DMSO (Vehicle).

Extract of *A. monticola* affects the PI3K/AKT signalling pathway and negatively regulates PPARγ and C/EBPα. The expression of *CEBPA* and *PPARG* is reduced upon treatment with ALM, AST and QUE in human SGBS adipocytes. Furthermore, the expression of *ADIPOQ* and *SREBP* is suppressed in a dose-dependent manner following the application of ALM extract. Furthermore, the expression of the lipogenic genes *ACC* and *FASN* is significantly suppressed upon treatment with the highest concentration of ALM, suggesting disruption of lipogenic signalling pathways. It is interesting to note that the expression of *ACC*, *ADIPOQ* and *FASN* is reduced upon administration of AST and QUE, but no change is observed in *SREBP*, which acts as their regulator.

The expression of *PPARG*, *ADIPOQ* and *ACC* is significantly reduced in all tested samples (ALM, AST, QUE). The expression of the *FASN* gene is reduced in samples treated with ALM 25 μg/mL, AST 5, 10, 25 μM and QUE 5 μM. The same effect was observed for *CEBPA*, with the exception of treatments with ALM 5 μg/mL and QUE 5 μM.

3.3. Protein detection by Western blot analysis – *A. monticola* and pure substances

Gene expression analysis confirms a concentration-dependent inhibitory effect of the ALM extract on gene expression. Despite the fact that AST and QUE did not affect lipid accumulation in the ORO assay (Figure 6C), the RT-qPCR results suggest that both compounds interfere with transcriptional regulation during adipogenesis. It could therefore be assumed that AST and QUE contribute to the observed anti-adipogenic effect of the ALM extract.

The ALM affects the PI3K/AKT signalling pathway and negatively regulates PPARγ and C/EBPα. Adipogenic differentiation is initiated in preadipocytes upon stimulation by external signals such as insulin, cortisol or other growth factors. The insulin signal is transmitted *via* the INSR and activates the PI3K/AKT pathway to induce pro-adipogenic transcription factors, which direct the cellular pathway towards adipogenesis (Ortega-Molina et al., 2015; Huang et al., 2018). Consequently, the regulation of adipogenic differentiation is mediated by CEBPα and PPARγ (Liu et al., 2014; Park et al., 2016; Vasileva et al., 2021; Zhou et al., 2024). Their overexpression leads to the subsequent activation of SREBP-1, which in turn increases lipid biosynthesis via ACC and FASN. All of this leads to the stimulation of lipid droplet formation.

In parallel with this process, levels of adiponectin, which is a key adipogenic marker of the mature adipocyte, increase (Arner et al., 2019; Liu et al., 2014; Xu et al., 2020). To further elucidate the molecular mechanism of action of ALM and the selected pure compounds AST and QUE, the protein expression of PPARγ, C/EBPα and adiponectin, as key adipogenic markers, was investigated by Western blot. Consistent with the crucial role of PI3K/AKT signalling in adipocyte differentiation and the results of the docking analysis, an increase in the levels of these protein molecules in the cells was observed (Figure 7A).

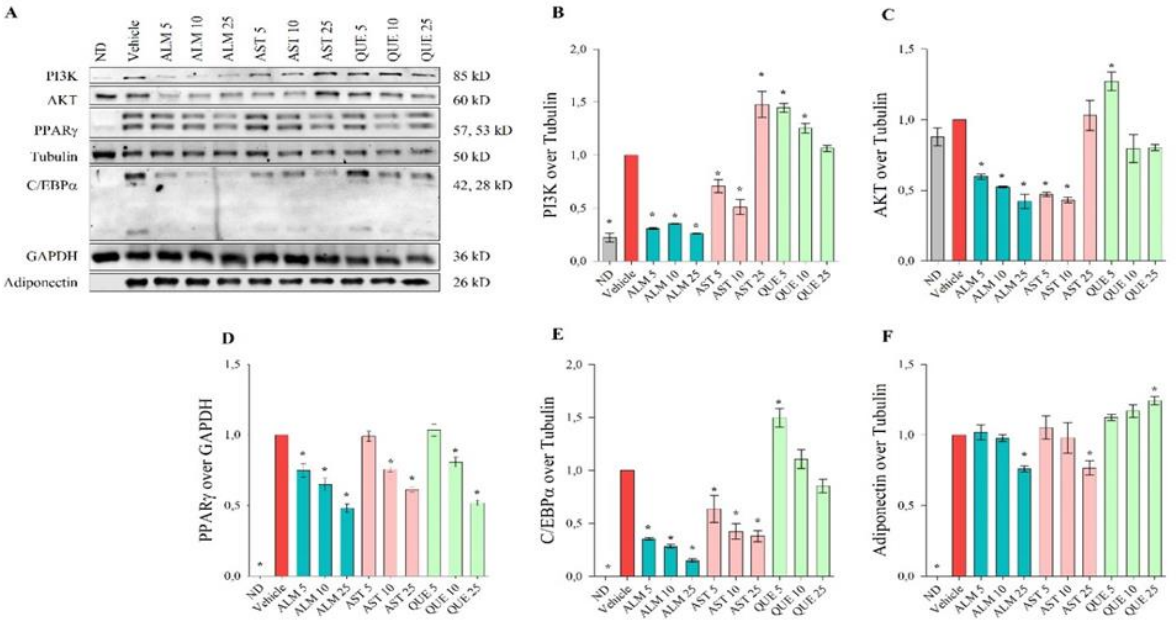

Figure 8. Extracts of *A. monticola* (ALM), astragalin (AST) and quercitrin (QUE) reduce the protein levels of key adipogenic factors in human adipocytes. Representative images from Western blot analysis (A). Relative levels of PI3K; (B), AKT (C), PPARγ (D), C/EBPα (E), and adiponectin (F). Tubulin (TUBB) and glyceraldehyde-3-phosphate dehydrogenase (GAPDH) were used as reference proteins. Results are expressed as mean ± SEM and are representative of three independent experiments. * $p < 0.05$ compared with the vehicle group – 0.2% DMSO (Vehicle).

A negative effect was observed on both PI3K (Figure 8B) and AKT (Figure 8C) by ALM in a concentration-dependent manner. These results are consistent with the results from docking simulations, ORO analysis and gene expression studies. Of interest is the effect of AST treatments, which appears to be bidirectional. Lower concentrations of AST (up to 10 μM) caused a decrease in PI3K and AKT levels, whilst the highest concentration increased both proteins. PI3K and AKT levels were slightly increased as a result of QUE exposure. Consistent

with the analysis of mRNA expression, the levels of PPARγ, C/EBPα and adiponectin proteins were reduced in a concentration-dependent manner upon treatment with ALM (Figure 8). Furthermore, it was found that AST inhibits PPARγ (Figure 8D) and C/EBPα (Figure 8E) in a manner consistent with that observed for their respective genes (Figures 8C and 8E). However, with regard to adiponectin (Figure 8F), treatment with AST moderately reduced levels, and this occurred at the highest concentration (25 μM). Interestingly, QUE increases the expression of C/EBPα and adiponectin (Figure 8F) and weakly inhibits PPARγ when applied at a concentration of 25 μM (Figure 8D).

Overall, these results indicate that ALM suppresses the process of adipogenesis by modulating the PI3K/AKT signalling pathway, thereby inhibiting the adipogenic markers PPARγ, C/EBPα and adiponectin. Furthermore, both AST and QUE affect the protein levels of PPARγ, C/EBPα and adiponectin to varying degrees, supporting the hypothesis that they play a role in the extract's overall anti-adipogenic action.

The data obtained from the computer docking simulation, gene expression analysis and changes in the levels of the target proteins provide evidence for the potential mechanisms of the anti-adipogenic effect of ALM and its secondary metabolite AST. The results of the Western blot analysis showed that the effect of ALM is most likely mediated through inhibition of PI3K/AKT signalling. These data provide grounds for proposing a mechanistic hypothesis of direct inhibitory activity of ALM against C/EBPα and PPARγ, leading to a reduction in adiponectin levels. Similarly, AST reduces C/EBPα and PPARγ and, to a lesser extent, those of adiponectin, PI3K and AKT. It could therefore be suggested that the anti-adipogenic effect of AST is more likely related to direct interaction with PPARγ or C/EBPα than to modulation of PI3K.

4. Anti-adipogenic effect in an *in vitro* model of human adipocytes treated with *O. spinosa* extract and its secondary metabolites

4.1. Adipogenesis and lipolysis – *O. spinosa* and secondary metabolites

To assess lipid accumulation, differentiated adipocytes treated with *O. spinosa* (5, 10 and 25 μg/mL), ONON (5, 10 and 25 μM) or MACK (5, 10, 25 and 50 μM). Representative images of stained adipocytes (Figure 9A), as well as the quantitative analysis of the results (Figure 9B), demonstrate modulation of adipogenesis in all treatments. An increase in lipid accumulation was observed to 123.25, 113.6 and 113.29% for OSR at 5, 10 and 25 μg/mL, respectively. In

contrast to the effect induced by the blackthorn extract, ONON significantly reduced lipid accumulation by 74.3, 77.85 and 77.63% at 5, 10 and 25 μM. In addition, MACK reduced lipid accumulation in a concentration-dependent manner to 70.46%, 74.09%, 62.70% and 54.52% for 5, 10, 25 and 50 μM, respectively.

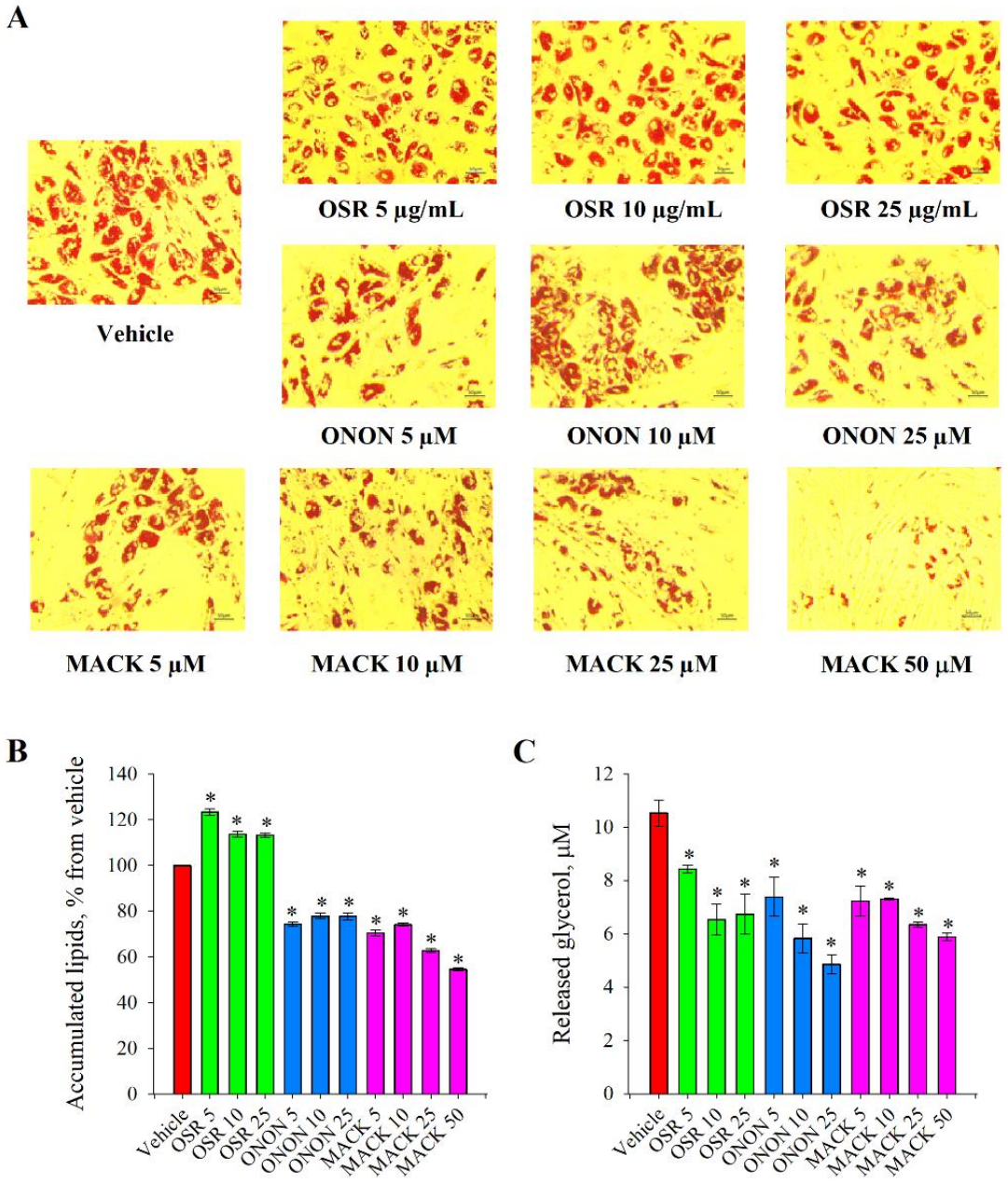

Figure 9. Modulation of adipogenesis was observed in all treatments with *O. spinosa* extract (OSR) and the pure compounds ononin (ONON) and maackiain (MACK). Lipid content, expressed as a percentage of the vehicle control group, in adipocytes treated with OSR at 5, 10 and 25 μg/mL, ononin (ONON) at 5, 10 and 25 μM, or maackiain (MACK) at 5, 10, 25 and 50

μM, as determined by ORO analysis (B). Representative images (magnification ×20) of all experimental groups following ORO staining (A). Assessment of free glycerol in the culture medium on day 9 of differentiation (C). Data are expressed as mean ± SEM; each experimental group consists of six technical replicates across three independent biological experiments. * $p < 0.05$ compared with the vehicle group.

The hydrolysis of triglycerides leads to the release of free fatty acids and glycerol. Given that free glycerol is a product of adipolysis, measuring its concentration in the culture medium has been used as an indicator of basal (unstimulated) lipolysis. The OSR extract and its secondary metabolites used in this study significantly reduced the amount of glycerol secreted by the cells (Figure 9C). A reduction in glycerol release was observed with OSR (8.43, 6.53 and 6.73 μM at 5, 10 and 25 μg/mL, respectively). Lipolysis was dose-dependently inhibited by ONON and MACK, with the most significant effect observed following treatment with 25 μM ONON (4.84 μM) and 50 μM MACK (5.87 μM). This effect may contribute to the beneficial impact of the tested compounds on improving metabolic dysregulation during obesity.

It is important to note that adipogenesis was significantly inhibited by ONON and MACK and moderately stimulated by OSR, with the highest inhibitory effect observed at 50 μM MACK.

4.2. Gene expression analysis by RT-qPCR – *O. spinosa* and pure compounds

Ononin and maackiain influence the expression of key transcription factors from the early and terminal phases of adipogenic differentiation.

The selected secondary metabolites identified in the *O. spinosa* root extract, namely ONON and MACK, effectively alter the adipogenic and lipolytic capacity of adipocytes. To further elucidate the main pathways involved, the relative expression of messenger RNA of key transcription factors associated with the initiation of adipogenic differentiation was investigated. Selected adipogenic and lipogenic genes, such as *ACC*, *ADIPOQ*, *AKT*, *SERBP1*, *CEBPA*, *PI3KCA*, *PPARG*, *SIRT1* and *AMPK*, were examined on day 9 adipocyte differentiation (Figure 10A).

To examine the effect on the early stage of adipogenic differentiation, the relative gene expression of CEBPB and CEBPD was analysed as markers (Choi et al., 2020, Jo et al., 2019, Mandl et al., 2019, Moseti et al., 2016) on day 3 of differentiation in adipocytes treated with the highest experimental concentrations. A significant downregulation of CEBPB (Figure 10B) and upregulation of CEBPD (Figure 10C) were observed compared to the control group.

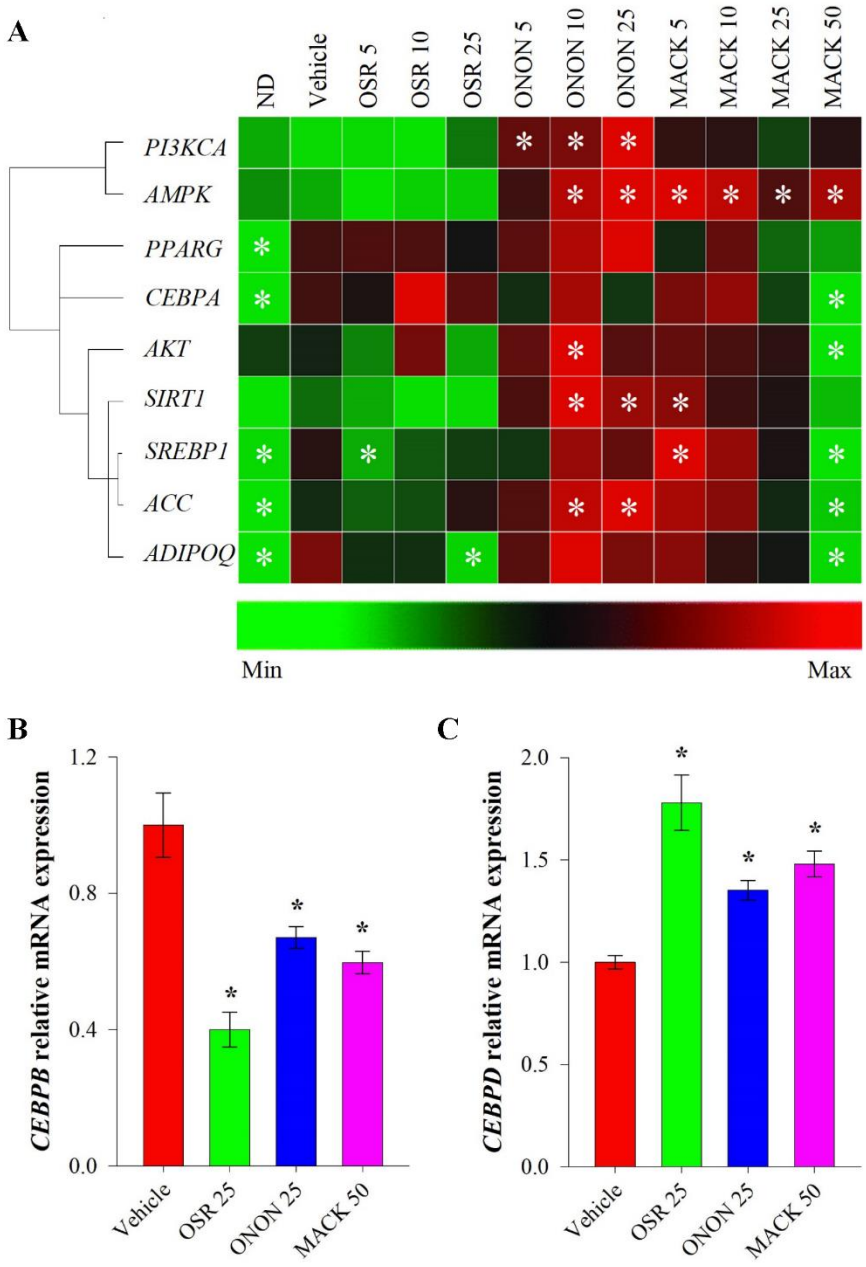

Figure 10. Heat map and dendrogram of relative gene expression clusters (A) for all treatments on the 9 th day of differentiation, and the relative gene expression of CEBPB (B) and CEBPD (C) in treatments with the highest concentrations of OSR, ONON, and MACK on the 3 th day of differentiation, performed by RT-qPCR analysis. The data are representative of three

independent replicates (mean ± SEM), *p < 0.05 compared to the control group. The mRNA expression levels of the target genes were normalised against those obtained for *RPL13A* and *TUBB*.

These results suggest that OSR and its secondary metabolites ONON and MACK are involved in the regulation of adipogenic differentiation as early as its initial phase.

RT-qPCR analysis showed that OSR significantly reduced the mRNA expression of the genes encoding adiponectin – *ADIPOQ* (OSR 25 μg/mL) and *SERBP1* (OSR 5 μg/mL). Treatment with 50 μM MACK largely inhibited the expression of *ADIPOQ*, *ACC*, *SERBP1*, *CEBPA* and *AKT*, and increased the expression of *AMPK*. Increased expression of *AKT* was demonstrated by 10 μM ONON. In the groups treated with 10 and 25 μM ONON, the gene expression of *PI3KCA, SIRT1, AMPK and ACC* was increased in a statistically significant manner.

The direct interaction between *SIRT1* and *AMPK* is largely associated with the regulation of lipid metabolism. For example, *SIRT1* stimulates the phosphorylation of *AMPK* and the subsequent inhibition of adipogenesis and lipogenesis by downregulating the expression of lipogenic genes (Lee et al., 2019; Liou et al., 2020). The present experiment showed that ONON 10, 25 μM and MACK 5, 10, 25, 50 μM increase *AMPK* expression. Furthermore, the expression of *SIRT1* mRNA was analysed to determine whether it contributes to the effect of ONON and MACK on adipocyte differentiation and lipid metabolism.

It is suggested that ONON 10, 25 μM and MACK 5 μM reduce lipid accumulation by increasing the expression of *SIRT1* and *AMPK* messenger RNA. The significant anti-adipogenic effect of MACK 50 μM is accompanied by suppressed gene expression of key transcription factors such as *SERBP1*, *CEBPA* and *ACC*.

In summary, all data from the gene expression analysis indicate that MACK and ONON influence the expression of numerous transcription factors in both the early and terminal phases of adipogenic differentiation.

4.4 Determination of protein levels by Western blot analysis of *O. spinosa* and pure compounds

Adipocyte differentiation is a complex and precisely regulated process triggered by various stimuli, the early phase of which is coordinated by C/EBPβ and C/EBPδ, whilst the terminal phase is directed by the two main transcription factors – C/EBPα and PPARγ. Adipogenesis

induced by insulin and insulin-like growth factor 1 (IGF-1) is mediated by the PI3K/AKT signalling pathway (Mandl et al., 2019). The metabolic function of phosphorylated AMPK is associated with the inhibition of adipogenic markers and, simultaneously, the enhancement of fatty acid oxidation (Jo et al., 2019). Modulation of this mechanism is a promising approach for identifying potential compounds with anti-adipogenic activity. To support the data from the RT-qPCR analysis, a panel of proteins from several key regulators of adipogenesis (PPARγ, AKT, AMPK, pAMPK, adiponectin, C/EBPα, PI3K) was analysed.

Docking simulations suggest a probable interaction between ONON or MACK with PI3K, PPARγ and AMPK at the protein level. Immunoblot analysis data revealed inhibition of PI3K by ONON at 5 and 25 μM and by MACK at 5, 10 and 50 μM (Figure 11D). A reduction in PPARγ protein levels was achieved upon treatment with ONON at 25 μM and MACK at 5 and 50 μM (Figure 11C). However, protein levels of AMPK (Figure 11F) and its active form pAMPK (Figure 11G) were moderately reduced upon treatment with ONON 5 and 10 μM and MACK 5 and 25 μM. Consistent with the RT-qPCR analysis, 50 μM MACK significantly reduced the levels of C/EBPα protein (Figure 11B).

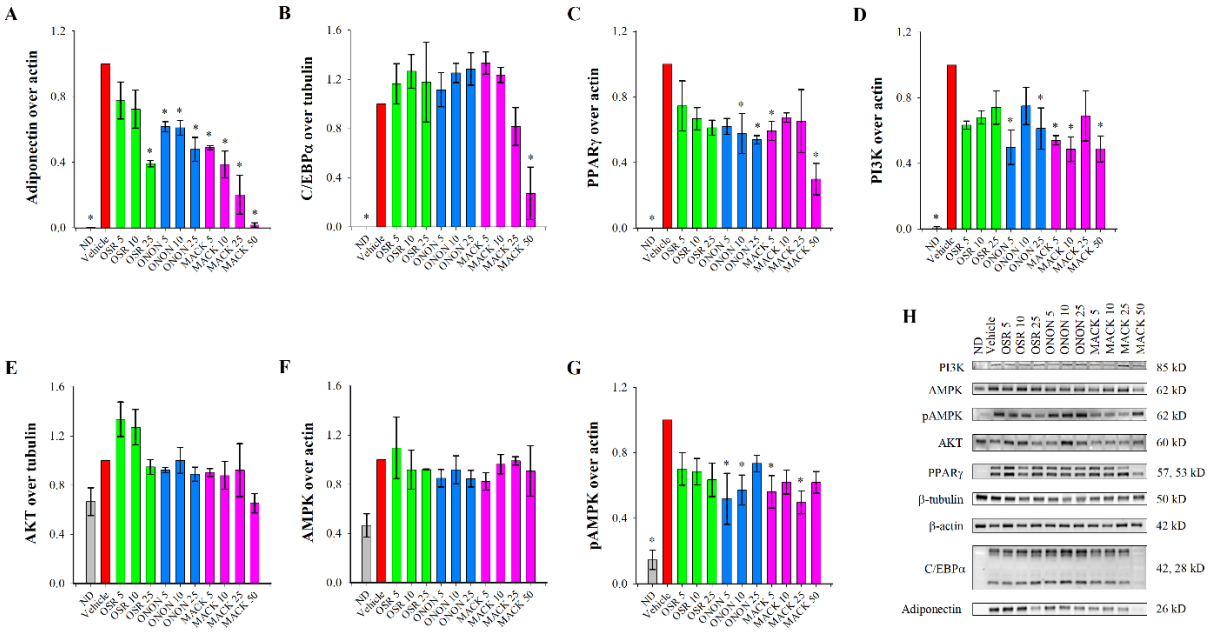

Figure 11. Extract of *O. spinosa* (OSR), ononin (ONON) and maackiain (MACK) influence the protein expression of key adipogenic regulators. Protein levels of adiponectin (A), C/EBPα (B), PPARγ (C), PI3K (D), AKT (E), AMPK (F), pAMPK (G), normalised against β-actin or β-tubulin. Representative immunoblot images (H). Results are from three independent experiments, expressed as mean ± SEM, *$p < 0.05$ compared to the control group.

Adiponectin levels as one of the markers of adipocyte maturation (Moseti et al., 2016) were significantly reduced upon treatment with OSR 25 μg/mL, as well as with ONON and MACK at all applied concentrations (Figure 11A). Despite the confirmed effect of inhibiting adipocyte differentiation, adiponectin levels must be closely monitored, as there is evidence that they correlate with insulin sensitivity in adipose tissue (Moseti et al., 2016).

Maackiain, at the highest applied concentration (50 μM), significantly reduced the levels of the key adipogenesis regulators PPARγ and C/EBPα. The immunoblot results support the claim that MACK inhibits adipogenesis *via* the PPARγ/C/EBPα signalling pathway. The immunoblot results support the hypothesis that MACK inhibits adipogenesis *via* the PPARγ/C/EBPα signalling pathway.

Based on the results of the *in vitro* anti-adipogenic assays, maackiain was selected as the most promising secondary metabolite for subsequent *in vivo* validation of its anti-adipogenic effect.

5. Validation of the established *in vitro* anti-adipogenic activity of maackiain in an *in vivo* model of obesity in *C. elegans* nematodes

5.1. Determination of the effect of maackiain on viability and phenotypic parameters in Nematodes

The lack of change in nematode viability upon application of MACK at concentrations up to 200 μM confirms its safety (Figure 12A). Changes in motor activity in response to external stimuls are necessary for escape responses, foraging and other complex behaviours. In this experiment, the effect on nematode motility following treatment with MACK at concentrations of 25, 50 and 100 μM was investigated (Figure 12B).

Studies of chemotaxis in *C. elegans* contribute to understanding of the neural mechanisms involved in behavioural responses triggered by environmental signals. Nematodes use their chemosensory system to search for food sources, avoid harmful substances and find mates. During the nematode experiment, the chemotaxis index was calculated as an indicator of the degree of attraction to MACK. The test was conducted using the highest concentration of MACK (100 μM, Figure 12B), with the results showing that the nematodes were most strongly attracted to MACK.

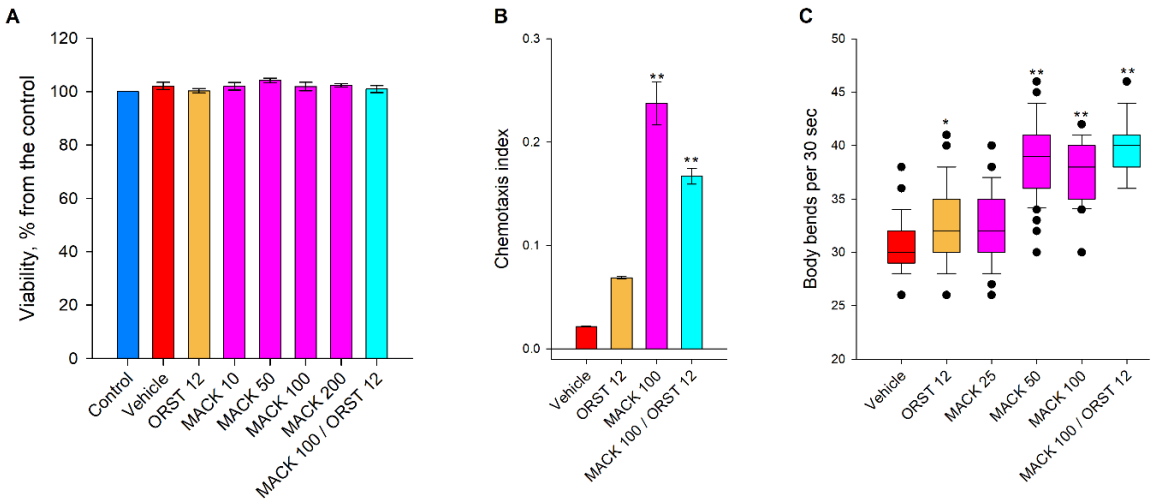

Figure 12. Viability and phenotypic parameters in *C. elegans.* Nematode viability (A) presented as a percentage of the control group after 48 hours of treatment with , orlistat (ORST), increasing concentrations of MACK, and a hybrid combination of ORST/MACK. Results are shown as mean ± SEM based on three replicates. Statistical significance relative to the control group is indicated as $p < 0.05$. Effect of MACK (100 μM), ORST (12 μM) and their hybrid combination on the chemotaxis index (B). Motor activity of nematodes (C), presented as the number of bends per 30 seconds following treatment with MACK at concentrations of 25, 50, 100 μM, ORST (12 μM) and a combination of ORST 12 μM/MACK 100 μM. Data from three independent experiments are presented as mean ± SEM, *$p < 0.05$, **$p < 0.001$ and compared with the vehicle control group.

5.2. Assessment of lipid accumulation in nematodes

The change in lipid accumulation in the *in vivo* model used was assessed by Nile red staining, comparing groups of nematodes cultured with and without glucose (Figure 13).

Confocal fluorescence images were captured from the prepared microscope slides of each of the nematode groups. The results show that treatment with MACK at a concentration of 100 μM and the combination of MACK 100 μM/ORST 12 μM most significantly reduced lipid accumulation in L4-stage nematodes.

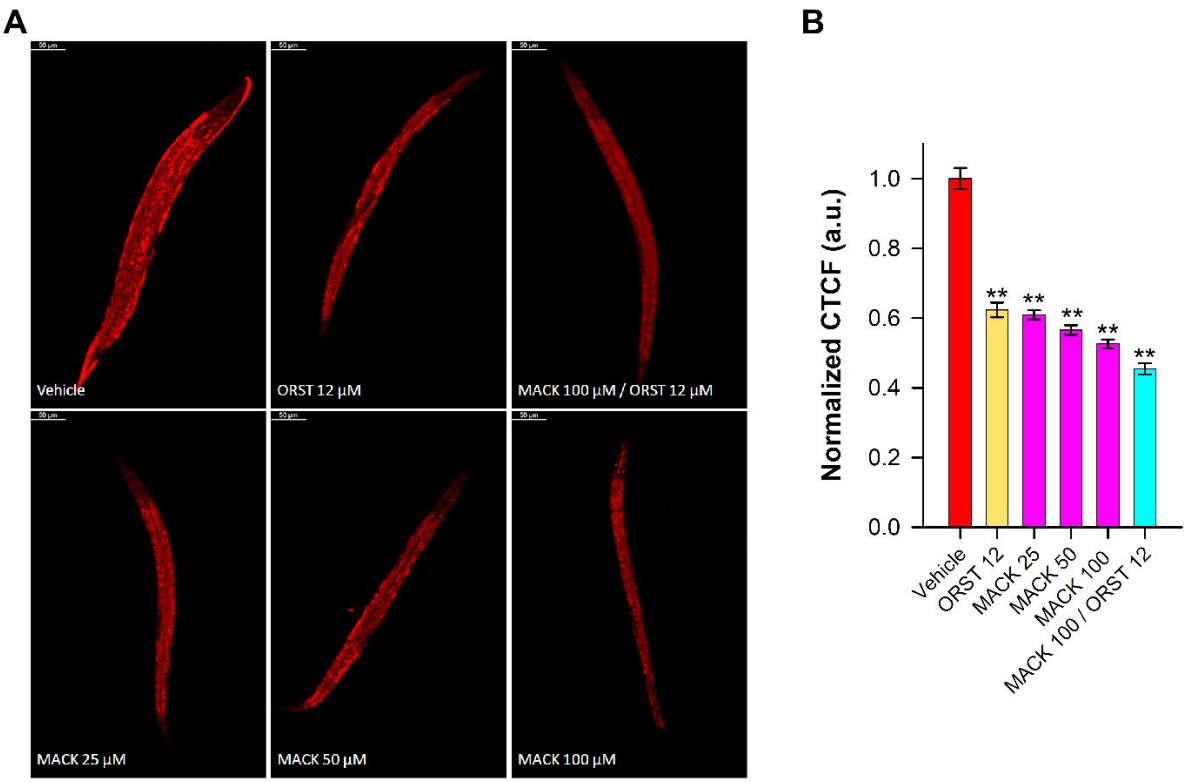

Figure 13. Representative confocal fluorescence images of nematodes treated with MACK at concentrations of 25 µM, 50 µM, 100 µM, a combination of MACK/ORST, 12 µM orlistat and the control (Vehicle; A).Quantification of fluorescence intensity in nematodes treated with MACK at concentrations of 25 µM, 50 µM, 100 µM, 12 µM orlistat (ORST) and a combination of MACK/ORST, normalised against a control group with glucose included in the culture medium and presented as corrected total cell fluorescence (CTCF, B). Data are presented as mean ± SEM **$p < 0.001$ compared to the control group.

5.3. Identification of key genes for lipid metabolism in *C. elegans*

Lipid metabolism in *C. elegans* involves numerous complexly regulated processes. In the present study, the expression profile of key transcription factors associated with the activation of lipid biosynthesis, namely *sbp-1* and *cebp-2*, was investigated. Furthermore, as a functional homologue of human PPARs, the expression of the transcription factor *nhr-49* was determined; this factor supports two distinct aspects of lipid metabolism, fatty acid desaturation and β-oxidation (Schwartz et al., 2015; Moreno-Arriola et al., 2016; Goh et al., 2018; Nunez et al., 2023). The relative RNA expression of *aak-2*, an AMPK orthologue (Li et al., 2020; Jeong et al., 2023), as well as *sir-2.1* and *mdt-15*, to determine whether treatment with MACK affects nutrient and energy metabolism-related signalling pathways. It is known that activation of these

pathways has a beneficial effect on lipid metabolism and is therefore associated with the mimicry of calorie restriction (Moreno-Arriola et al., 2016; Weir et al., 2017; Madeo et al., 2019).

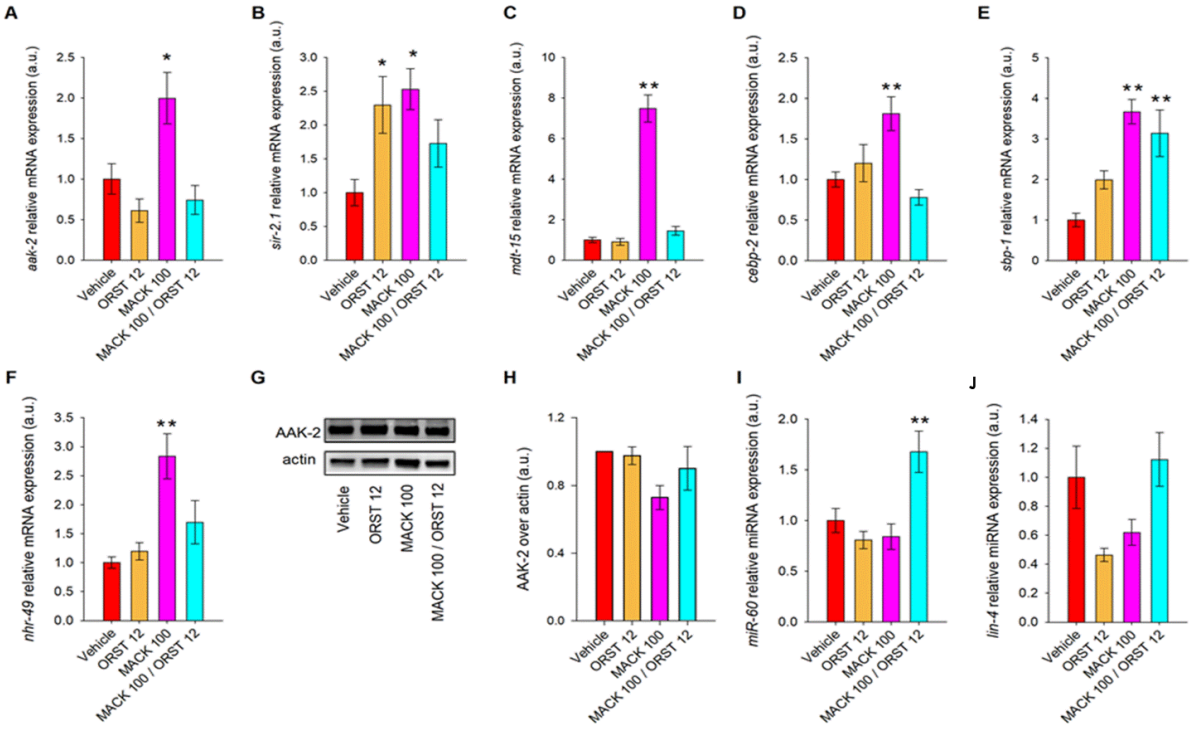

Figure 14. Determination of the relative expression of mRNAs, microRNAs and proteins of key genes involved in lipid metabolism in an obesity model in nematodes treated with MACK at a concentration of 100 µM, a combination of MACK/ORST and 12 µM orlistat (ORST). Gene expression of *aak-2* (A), *sir-2.1* (B), *mdt-15* (C), *cebp-2* (D), *sbp-1* (E), *nhr-49* (F) normalised against the control group. Protein levels of phosphorylated AAK-2 (G) normalised to actin; expression of microRNAs: *miR-60* (I) and *lin-4* (J) normalised to the vehicle group (Vehicle). Data are presented as mean ± SEM *p < 0.05, **p < 0.001 compared to the vehicle group.

Treatment with maackiain resulted in a significant and concentration-dependent reduction in triglyceride accumulation in glucose-fed nematodes. Analysis of the relative expression of nematode mRNAs and microRNAs in nematodes treated with MACK (100 µM), ORST (12 µM) or the MACK/ORST hybrid combination (100/12 µM) elucidates the molecular mechanism involved in the observed anti-obesogenic effect (Figure 14).

A single treatment with MACK at the highest applied concentration (100 µM) significantly up-regulated aak-2, sir-2.1, mdt-15, nhr-49, cebp-2 and sbp-1 (Figure 14A–F) in

compared to the vehicle. Treatment with orlistat induces significant regulation of sir-2.1 (Figure 14B), whilst its combination with MACK increases the relative expression of sbp-1 (Figure 14E). The observed change in the relative expression of selected participants in lipid metabolism, such as aak-2 and sir-2.1 in nematodes, indicated that MACK activates the signalling pathways involved in fatty acid oxidation, mitochondrial biogenesis and energy expenditure, which are closely associated with calorie restriction.

The activation of AAK-2/AMPK in *C. elegans* is associated with food-restriction-dependent lifespan extension through the remodelling of mitochondrial function in peripheral tissues, increased energy expenditure and the promotion of healthy ageing (Schwartz et al., 2015; Weir et al., 2017; Zhang et al., 2019; Jeong et al., 2023). The observed transcriptional activation of *AAK-2* upon treatment with MACK confirmed the need to analyse AMPK phosphorylation levels at Thr172, a site associated with increased activity, in the glucose-induced *C. elegans* model (Figure 14G,H). Immunoblot analysis at the selected time point showed no altered phosphorylation of AAK-2 in either the MACK or the MACK/ORST combination.

Subsequent assessment of the relative expression of microRNAs was used to obtain a broader picture of gene expression regulation during the experimental treatment of *C. elegans* fed with glucose. Recent studies have focused on investigating the potential of natural compounds to modulate cancer-associated microRNAs, which could also be relevant to the study of obesity (Chen et al., 2005; Kato et al., 2016; Shamsuzzama et al., 2017; Zhang et al., 2020; Brosnan et al., 2021). In particular, several microRNAs such as *mir-60* and *lin-4* in *C. elegans* are associated with lipid metabolism and ageing. Furthermore, *mir-60* is expressed exclusively in the nematode gut, influencing their response to oxidative stress, nutrient uptake and recovery following food deprivation (Kato et al., 2016; Zhang et al., 2020; Brosnan et al., 2021).

The results of RT-qPCR show that only treatment with the MACK/ORST hybrid combination (100/12 μM) leads to an increase in *miR-60* expression (Figure 14I). Interestingly, earlier studies have established a link between *miR-60* downregulation and lipid reduction (Brosnan et al., 2021). However, our findings suggest that increased expression of this microRNA may also play a role in the mechanisms of lipid metabolism . In our study, *lin-4* was unaffected by any of the experimental treatments (Figure 14J). It is therefore reasonable to assume that the effect of the hybrid combination on lipids is likely unrelated to *lin-4*.

V. DISCUSSION

1. The PI3K/AKT signalling pathway is key to the anti-adipogenic effect of A. Monticola and its secondary metabolites

The development of obesity correlates with the regulation of body metabolism *via* the function of adipose tissue. It is therefore of great importance to identify bioactive substances whose effect targets adipocyte function in order to prevent and control this complex metabolic disorder.

The PI3K/AKT signalling pathway in adipocytes is responsible for initiating differentiation and lipid biosynthesis. One of the key substrates for AKT-related lipid metabolism is SREBP-1, which regulates fatty acid synthesis and cholesterol-related genes (Huang et al., 2018). Once preadipocytes enter the process of adipogenic transformation, the expression of PPARγ and C/EBPα activates a transcriptional cascade that initiates the expression of genes such as SREBP-1, ACC, FASN and adiponectin, which are considered adipocyte markers (Mandl et al., 2019; Vasileva et al., 2021).

The effects of flavonoids in diabetes and obesity are achieved through the modulation of key signalling pathways, thereby improving glucose metabolism and transport in pancreatic β-cells, hepatocytes, adipocytes and skeletal myofibrils (Goto et al., 2012; Hur et al., 2020; Wu et al., 2020). Metabolic profiling based on NMR spectroscopy identified the ALM as a source of various flavonoids and flavonoid glycosides, such as AST and QUE. Several previous studies report that AST regulates lipogenesis and fat accumulation in 3T3-1L adipocytes by suppressing the expression of PPARγ, C/EBPα, FASN and leptin mRNAs (Swamy et al., 2020; Wu et al., 2020). Similarly, ALM has demonstrated a significant effect against hepatic fat accumulation and a reduction in inflammatory markers in various models of liver damage (Roman Junior et al., 2015; Hur et al., 2020).

This experiment revealed that ALM extract can inhibit the differentiation and lipid accumulation in human adipocytes, and that its active components, AST and QUE, contribute at least in part to the observed anti-adipogenic effect. ALM extract reduces the expression of various genes and proteins associated with adipogenesis and inhibits the differentiation of human preadipocytes. ALM extract suppresses PI3K/AKT-mediated signalling cascades that induce preadipocyte proliferation; this effect may be due to inhibition of INSR kinase *via* direct binding of AST or another ALM compound to active PI3K. Protein levels of PI3K and AKT are reduced in a concentration-dependent manner following treatment with ALM. However, consistent with the docking simulation, the tests indicate that pure AST has bidirectional effects on the PI3K/AKT signalling pathway. This suggests that AST may exert a bidirectional

regulatory effect on the PI3K/AKT signalling pathway in human adipocytes, with the critical concentration for this bidirectional regulation lying between 10–25 μM. Similarly, the anti-adipogenic effect of cocoa polyphenols in adipocytes from rats and mice on an obesity-inducing diet was confirmed in a previous study (Min et al., 2013). The authors provided evidence that cocoa polyphenols directly inhibit INSR and subsequently suppress both ERK- and PI3K/AKT-mediated signalling cascades (Min et al., 2013).

Insulin signalling plays a critical role in lipid storage in adipose tissue, as well as in glucose homeostasis. In the presence of insulin, INSR autophosphorylates and subsequently phosphorylates the IRS family, resulting in the activation of two major signalling pathways, Ras/MAPK and PI3K/AKT (Huang et al., 2018; Li et al., 2020b). The activation of IRS-1 promotes the phosphorylation of AKT, with activation occurring *via* a link between the regulatory subunit of PI3K and the phosphotyrosine residues of IRS-1. Subsequently, the PI3K/AKT signalling pathway participates in the initiation of differentiation *via* complex signalling cascades (Ortega-Molina et al., 2015; Huang et al., 2018). Consequently, the inhibitory effect of ALM on PI3K activity and its downstream signalling pathways (PI3K/AKT) appears to mediate this anti-adipogenic effect. At the same time, the PI3K/AKT pathway is also responsible for a wide range of metabolic functions in other tissues (Huang et al., 2018; Xu et al., 2020). Blocking INSR activity should be used with caution, as this may lead to adverse consequences, such as the development of insulin resistance. Previous studies have demonstrated that INSR activity is impaired in the skeletal muscles of individuals with obesity and diabetes; specific mice with liver INSR knockdown exhibit severe insulin resistance and glucose intolerance (Min et al., 2013; Li et al., 2020b; Xu et al., 2020). In this context, pure AST, which acts as a PI3K inhibitor, may also induce insulin resistance. Although insulin-mediated activation of the INSR is a major inducer of adipogenesis, insulin-like growth factor (IGF)-1 and the IGF-1 receptor (IGF1R) are other critical factors for initiating insulin-signalling *via* the activation of PI3K/AKT-mediated signalling cascades (Huang et al., 2018). It is likely that AST, QUE or other components of ALM interact with IGF1R, leading to the inhibition of adipogenesis without reducing the action of insulin. Further studies are needed to investigate whether ALM extract or its pure compounds protect against insulin resistance by increasing IGF1R activity or exert a direct inhibitory effect on the INSR. However, it was not possible to determine during the experiment whether ALM or AST improve insulin resistance, due to the fact that an *in vitro* model system was used. Another possible explanation could be that the inhibition of PI3K/AKT signalling observed with ALM and treatment with the pure

compound AST is tissue-specific, and therefore the potential effect on insulin sensitivity may vary across different cell types.

The transcription factors PPARγ and C/EBPα are continuously expressed in mature adipocytes (Aprile et al., 2018; Vasileva et al., 2021). In addition to modulating PI3K/AKT signalling, ALM and its pure components also inhibited adipocyte differentiation, as evidenced by a reduction in the expression of PPARγ and C/EBPα at both the gene and protein levels. The interaction of AST and QUE with PPARγ and/or C/EBPα was predicted by *in silico* simulation and further confirmed by analysis of gene and protein expression.

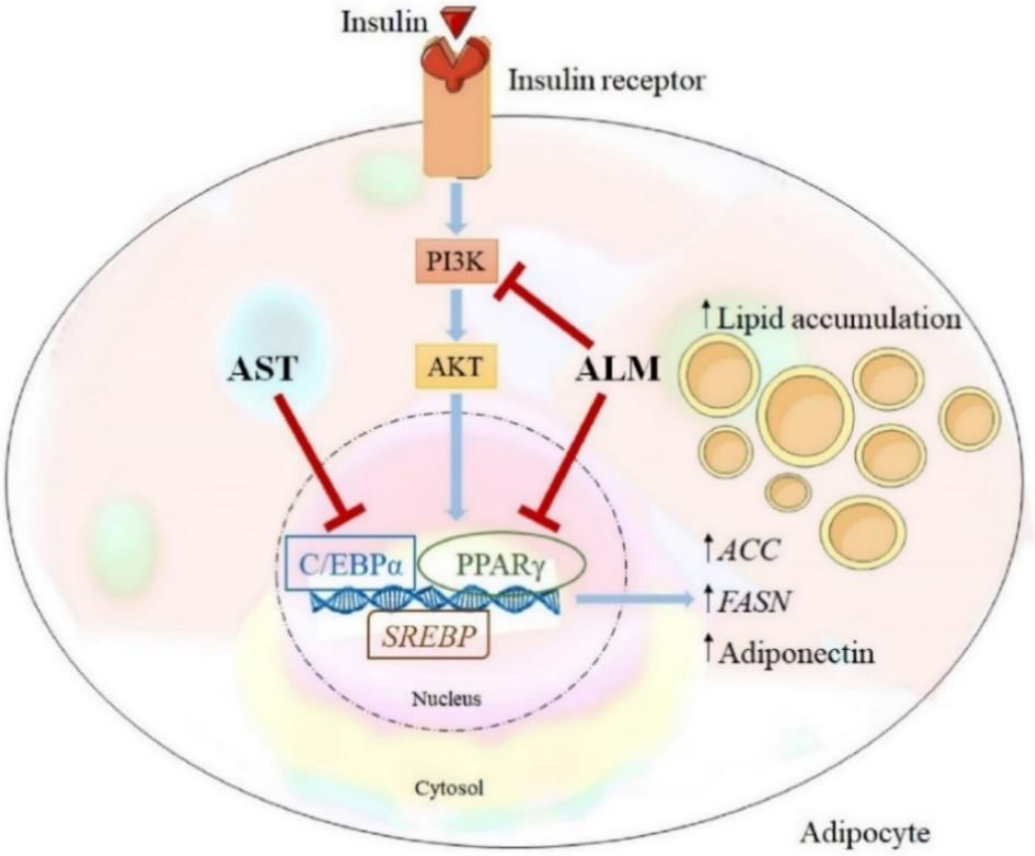

Figure 15. Proposed mechanism of action of the extract of the *A. monticola* (ALM) and astragalin (AST). Treatment with ALM reduced the levels of PPARγ and C/EBPα in human adipocytes, which is associated with the inhibition of the PI3K/AKT signalling pathway. In the case of treatment with AST, the anti-adipogenic effect is mediated via direct interaction with PPARγ and C/EBPα.

This experimental work provides a theoretical basis for the anti-adipogenic effect of ALM, mediated through modulation of the PI3K/AKT signalling pathway and PPARγ protein

levels. The identified pure compounds AST and QUE demonstrate potential for anti-adipogenic action through modulation of various signalling pathways. To further characterise these potential pharmacological effects of the ALM extract and its pure components, studies on other cell types and *in vivo* models of obesity should be conducted.

Furthermore, the present study provided evidence that ALM inhibits the early stage of adipogenesis in human adipocytes by inhibiting PI3K activity through direct binding. In addition, ALM exhibited anti-adipogenic activity, manifested as a reduction in intracellular lipids and enhanced lipolysis. Altered PPARγ, C/EBPα and adiponectin levels observed following ALM treatment in human adipocytes may be linked to the inhibition of the PI3K/AKT signalling pathway. It has also been established that the two pure compounds, AST and QUE, interfere with the adipogenic pathways under investigation to varying degrees (Figure 15). Overall, these findings suggest that ALM has the potential to prevent obesity, which requires further *in vivo* validation. It may be noted that the identified phytochemical composition of ALM is promising as a source of new bioactive compounds aimed at controlling obesity.

2. The anti-adipogenic activity of ononin and maackiain in human adipocytes is mediated via inhibition of PPARγ

Adipogenesis, as a finely regulated process, can be influenced by modulating the signalling molecules involved in it. Adipocyte differentiation is induced by insulin and IGF-1. Furthermore, insulin signalling is mediated via activation of the PI3K/AKT and RAS/MAPK pathways (Mandl et al., 2019). Once initiated, adipogenesis is regulated by the expression of C/EBPβ and C/EBPδ during the early adipogenic phase, followed by an increase in PPARγ and C/EBPα and the promotion of lipogenesis (Tang et al., 2021). The lipogenic transcription factor SREBP-1 and its target genes ACC and FASN (encoding key enzymes, Bertolio et al., 2019) play a major role in lipid biogenesis. This experiment confirmed that the selected secondary metabolites from OSR, ONON and MACK inhibit the process of adipogenic differentiation in human adipocytes. The results suggest a moderate effect on the early phase of adipogenic differentiation following treatment with OSR. Despite the reported moderate increase in lipid accumulation, observed in the Oil Red O analysis, neither the gene expression profile nor the number of copies of protein molecules in the cell of the investigated late-stage adipogenic markers were significantly affected by the application of OSR, with the exception of adiponectin at a concentration of 25 μg/mL.

Molecular interaction between PI3K and PPARγ and the two pure compounds was predicted to have a high affinity based on docking calculations and was further confirmed by immunoblotting results. The results obtained support the hypothesis that the inhibition of PI3K by ONON and MACK leads to changes in the expression levels of messenger RNA of early adipogenic markers, such as C/EBPβ and C/EBPδ. Maackian significantly inhibits adipogenesis and lipogenesis by reducing the expression of SREBP1 and ACC genes. Furthermore, MACK reduced the levels of the PI3K protein, considered a mediator of adipogenic transformation, and inhibited the expression of late-stage adipogenically specific transcription factors such as PPARγ, C/EBPα, as well as adiponectin in human adipocytes. Through a similar mechanism, ONON exerted its anti-adipogenic effect by reducing PI3K protein levels, increasing SIRT1 expression, and subsequently inhibiting PPARγ and adiponectin. The two secondary metabolites (ONON and MACK) inhibited PI3K, suggesting that the pure compounds affect the early stages of adipogenic differentiation. Adipogenesis was inhibited by MACK *via* PPARγ/C/EBPα signalling, whilst lipogenesis was negatively affected by downregulation of SREPB1 and its lipogenic genes. Unlike MACK, ONON exhibited an anti-adipogenic effect solely by upregulating SIRT1 and inhibiting PPARγ. Furthermore, ONON and MACK reduced adiponectin levels, which may ultimately be a secondary effect of PPARγ modulation.

Inhibition of adipocyte differentiation and modulation of lipolysis are potential molecular mechanisms in the treatment of obesity and its associated complications (Santos et al., 2021). The terminal differentiation of adipocytes is regulated by PPARγ and C/EBPα, whilst SREBP-1 is responsible for controlling lipogenesis. Furthermore, the transcriptional activity of PPARγ, along with adipogenesis, can be negatively affected by SIRT1 activation. In addition, successful reduction of excess adipose tissue is observed upon inhibition of the PI3K/AKT signalling pathway (Foukas et al., 2013; Jeffery et al., 2015; Ortega-Molina et al., 2015; Nagai et al., 2018), revealing another target for the treatment of obesity.

Root extravt of *O. spinosa* is rich in various classes of secondary metabolites (Abdesselem et al., 2016; Addotey et al., 2018). Based on data from the ethnopharmacological use of OSR extract for the treatment of metabolic disorders, including obesity, and the lack of scientific evidence regarding the effect of OSR on adipogenesis, the anti-adipogenic potential of OSR was investigated for the first time in an *in vitro* model of human adipocyte obesity. Analysis of the proton NMR spectra of OSR, in accordance with the literature, revealed the

presence of ononin, sativanon, onogenin, spinonin and maackiain as secondary metabolites (Gampe et al., 2016; Addotey et al., 2018). Further analysis of the 2D NMR spectra of the plant extract confirmed the presence of ONON and MACK, and these were selected for subsequent biological experiments alongside OSR. Schematic representation of the proposed anti-adipogenic mechanism of *O. spinosa* root extract, ONON and MACK (Figure 16).

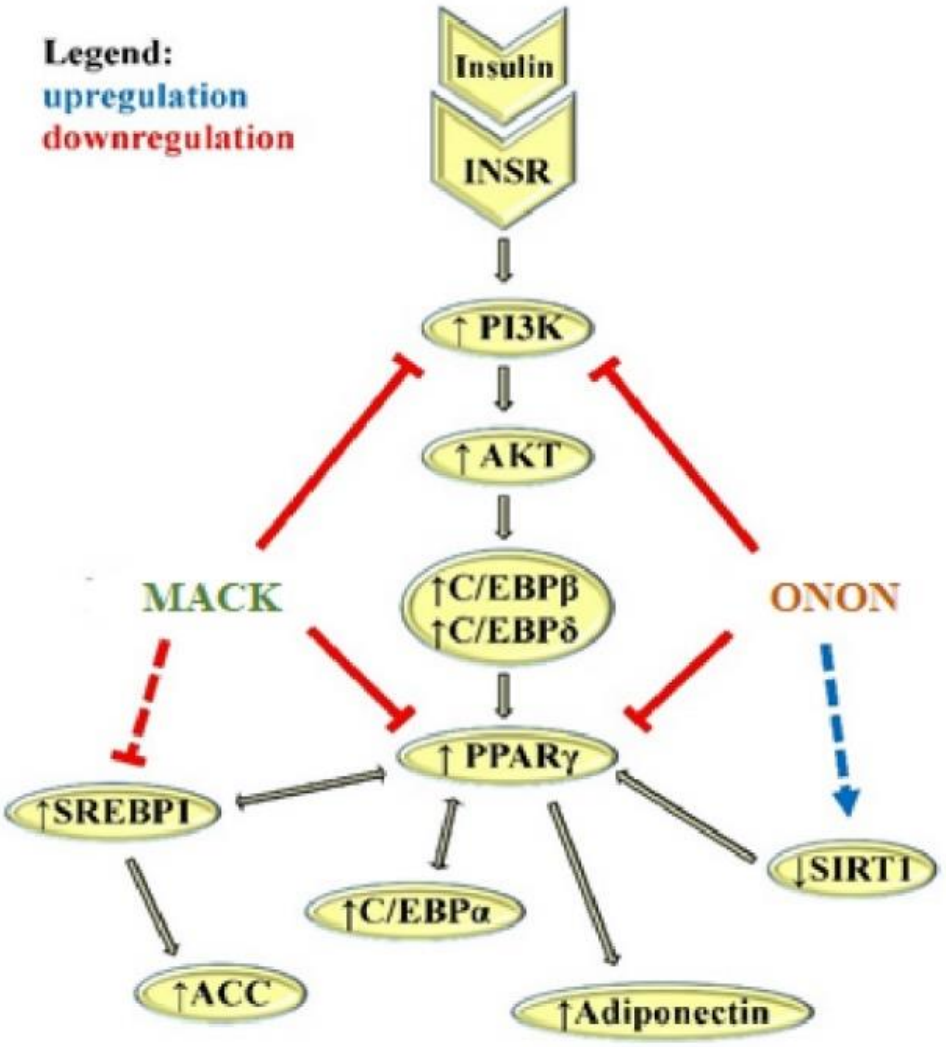

Figure 16. The cascade of adipogenic differentiation and proposed mechanisms of the anti-adipogenic and/or anti-lipogenic effects of ONON (ononin) and MACK (maackiain), identified in an extract from the root of *Ononis spinosa* L. Both ONON and MACK inhibit PI3K, a mediator of insulin signalling through INSR, and induce differentiation, leading to subsequent changes in the expression of C/EBPβ and δ. In addition, ONON activates SIRT1, which is an inhibitor of the transcription factor PPARγ key to terminal adipogenic differentiation and also suppresses the late adipogenic marker adiponectin. MACK influences adipogenesis by negatively regulating PPARγ and C/EBPα signalling, as well as that of adiponectin.

Subsequently, a suppression of lipogenesis mediated by SREBP-1 and its target enzyme ACC has been observed.

It is also of interest that OSR significantly stimulates adipogenesis, as demonstrated by lipid staining, and reduces lipid hydrolysis, as measured by the glycerol released into the culture medium. Furthermore, the results of analyses of relative mRNA and protein expression showed a moderate reduction in adiponectin following OSR treatment only at the highest applied concentration. These findings suggest that OSR does not act directly on the molecular regulatory pathways of adipogenic differentiation tested in our experimental work. Its apparent effect on improving metabolic disorders likely involves other molecular pathways or organs and tissues other than the adipose depot, which needs to be clarified in an in vivo model. Nevertheless, it is evident that both ONON and MACK induce a reduction in the rate of differentiation of human adipocytes, which supports the claim that OSR is a potential source of natural bioactive compounds against obesity.

The isoflavone glycoside ONON is found in many plants such as *Smilax scobinicaulis C.H.Wright, Millettia nitida Benth.* and species of Ononis (Gampe et al., 2016; 2018; Dong et al., 2017; Addotey et al., 2018; Yu et al., 2019; Chen et al., 2021; Gong et al., 2021). Although the literature data regarding its biological activity are limited, anti-inflammatory, anti-angiogenic and antiviral potential has been reported (Chen et al., 2012; Dong et al., 2017; Gong et al., 2021). It should be noted that ONON has not been investigated for anti-adipogenic effects to date, but its aglycone component (formononetin) has been reported to inhibit adipogenesis via the AMPK/β-catenin signalling pathway in an *in vivo* (mouse) model of obesity (Gautam et al., 2017). Similarly, in our study, adipocyte differentiation and lipolysis were significantly reduced in the presence of ONON. An *in silico* method predicted the possible interaction between ONON and the investigated protein targets such as AMPK, PI3K, PPARγ, C/EBPα and AKT. A reduced amount of PI3K and PPARγ proteins was observed *via* Western blot analysis as a result of treatment with ONON. The inhibition of PI3K by ONON may be the cause of the changes in the early-phase transcription factors C/EBPβ and δ. With regard to the level of AMPK protein, the results obtained are consistent with those of Gautam et al. (2017), as their study reported no change in total AMPK protein levels on day 9 of differentiation in mouse 3T3-L1 adipocytes. However, in contrast to this report, no increase in AMPK phosphorylation was observed. One very likely explanation is that formononetin may have a higher affinity for AMPK than ONON. It may also be that in human adipocytes, pAMPK

activation occurs prior to day 9, and therefore remains undetected in the current experimental setup. Upregulation of SIRT1 protects against metabolic damage through interaction with PPARγ (Perrini et al., 2019) and/or AMPK (Yao et al., 2018; Lee et al., 2019; Song et al., 2019; Liou et al., 2020). Furthermore, SIRT1 regulation is associated with reduced adipogenesis alongside increased osteogenesis (Song et al., 2019). Findings in this study support the claim that ONON regulates SIRT1 independently of AMPK activation, which may be crucial for the observed anti-adipogenic effect of ONON. Overall, the anti-obesogenic effect of ONON is likely mediated by the inhibition of PI3K and the promotion of SIRT1 regulation, with a subsequent reduction in PPARγ and adiponectin levels.

Maackiain is a pterocarpan reported to possess anti-allergic, anti-cancer, anti-inflammatory and antimicrobial activity, as well as inhibiting monoamine oxidase B (Nariai et al., 2015; Liu et al., 2020; Tsai et al., 2020). Furthermore, MACK inhibits the differentiation and bone-resorbing functions of mouse osteoclasts by suppressing the NF-κB signalling pathway (Liu et al., 2020). Given the mechanistic interrelationships between adipogenesis and osteogenesis (Muruganandan et al., 2020), the inhibition of bone resorption by MACK may share common molecular targets with the anti-adipogenic mechanism in adipocytes. In our study, a concentration-dependent reduction in lipid accumulation and triglyceride hydrolysis was observed following treatment with MACK. It also modulates the expression of key adipogenic transcription factors such as CEBPA, CEBPB, CEBPD and SERBP1, and the gene for the lipogenic enzyme ACC. Furthermore, MACK significantly increased the gene expression of AMPK. In support of the interactions simulated by docking, the same interactions between target proteins and MACK were confirmed by Western blotting, with a significant reduction in PI3K, PPARγ, C/EBPα and adiponectin observed. An exception is treatment with MACK, in which no changes were detected in either total AMPK or its phosphorylated form. Nevertheless, the strong binding affinity suggested by the docking results and the concentration-dependent transcriptional activation of this gene suggest that MACK warrants further investigation as an AMPK modulator. Similar to the proposed explanation for the effect of ONON on AMPK activity, it is possible that MACK also influences phosphorylation at a different time point during adipogenic transformation in human adipocytes. The data obtained indicate that MACK limits lipid accumulation by reducing lipogenesis through the suppression of SREBP-1 and ACC, as well as by inhibiting the adipogenesis-specific transcription factors PPARγ and C/EBPα in human adipocytes.

In summary of the experimental results, we can conclude that OSR does not significantly affect adipogenesis, whilst MACK and ONON significantly reduce lipid accumulation. The

inhibitory effect of MACK and ONON on lipid accumulation has been reported for the first time in an experiment with human adipocytes. The most likely mechanism of action of ONON is *via* PI3K inhibition, SIRT1 activation and subsequent inhibition of the PPARγ/adiponectin axis. The significant anti-adipogenic activity of MACK is mediated through the modulation of PI3K and PPARγ/C/EBPα signalling and the restriction of lipogenesis via the inhibition of SREBP-1 and ACC. Both compounds possess a significant anti-adipogenic effect that warrants *in vivo* validation.

In conclusion, of all the secondary metabolites studied, only MACK reduced lipid accumulation in a concentration-dependent manner. Furthermore, it modulated the expression of key adipogenic transcription factors such as CEBPA, CEBPB, CEBPD and SERBP1, and the gene for the lipogenic enzyme ACC. A significant reduction in PI3K, PPARγ, C/EBPα and adiponectin was confirmed at the protein level.

Based on the promising results of the tests conducted, its complex action and the fact that this is the first time evidence has been provided for the potential of MACK to inhibit adipogenesis, it was selected for subsequent *in vivo* validation of the results from the SGBS model.

3. Maackiain demonstrates anti-obesogenic activity *via* aak-2-mediated lipid reduction in *C. elegans*

The availability of a variety of cellular, molecular, genetic and behavioural analyses, and the similarity of key pathways regulating lipid metabolism, evolutionarily conserved between nematodes and humans, encourage the use of this model as a tool for obesity research (Dyczkowska et al., 2021).

Based on the results obtained from treatment with MACK in glucose-induced lipid accumulation in *C. elegans*, the molecular mechanism shown in Figure 17 is proposed. In the model organism used, a tendency towards overexpression of the mRNA of *cebp-2* and *sbp-1* is observed. The regulation of *sir-2.1* in nematodes indicates a potential co-interaction with *aak-2*, and defines their lipid-reducing effect via a mechanism mimicking calorie restriction. The PPAR homologue, *nhr-49,* is up-regulated in the present nematode experiment upon treatment with MACK, which is associated with *aak-2/sir-2.*1-dependent energy expenditure.

With regard to MACK, a study is cited that assessed its potential for alleviating symptoms of Parkinson's disease in a *C. elegans* model (Tsai et al., 2020). In response to calorie restriction, complex molecular mechanisms are initiated (Madeo et al., 2019). These complex pathways show a high degree of evolutionary conservation across different species.

Although the degree of genetic homology between humans and *C. elegans* is lower than that between humans and rodents, nematodes represent a physiologically suitable model organism for studying lipid metabolism due to their fully sequenced genome (Weir et al., 2017).

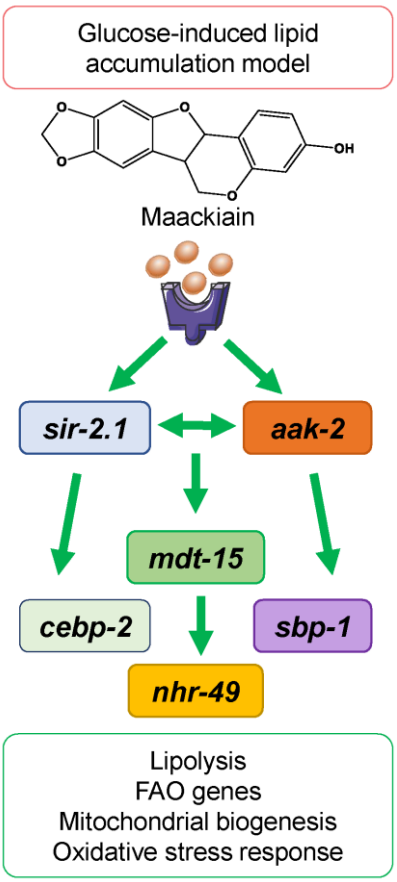

Figure 17. Mechanism of action of maackiain in a nematode obesity model. The effect of maackiain on lipid metabolism resembles that induced by certain calorie restriction mimetics. Mechanistically, maackiain acts on key sensory regulators in the nutrient and energy signalling network, such as *aak-2*, *sirt-2.1*, *nhr-49*, *cebp-2* and *sbp-1*.

For example, *C. elegans* is a recognised model for studying the role of AMPK and sirtuins in the regulation of cellular functions and their links to longevity and life extension, alongside their role in lipid metabolism (Guo et al., 2014; Farias-Pereira et al., 2019; Zhang et al., 2019). Similar to MACK, other bioactive molecules, such as caffeic acid, curcumin and gallic acid, have been shown to mitigate fat accumulation by modulating calorie restriction (Ma et al., 2015; Bakar et al., 2020; Yue et al., 2021). At the heart of this mechanism of action is AMPK/AAK-2, which is regulated in a similar manner following treatment with maackiain. The absence of AMPK/AAK-2 phosphorylation in the present experiment may be due to a different time point of phosphorylation peak, which has been reported for various activators

(Moreno-Arriola et al., 2016; Nunez et al., 2023). Furthermore, the correlation between the results in changes in locomotor activity and lipid staining suggests increased energy expenditure, a factor often associated with enhanced autophagy, regulated nutrient signalling and reduced oxidative stress (Sun et al., 2018). The observed effect may also influence the neuroendocrine network, particularly given that MACK, both alone and in combination with ORST, acts as an attractant for nematodes.

Recently, the approach of combining approved medicinal substances with bioactive compounds of natural origin has begun to be studied in depth. This approach aims to produce additional pharmacological effects, such as in the case of the senolytic combination of dasatinib and quercetin, which is currently undergoing clinical evaluation for musculoskeletal disorders (Taguchi et al., 2020; Novais et al., 2021; Islam et al., 2023). It is of interest that data from treatment with the hybrid combination of MACK/ORST show a superior effect in terms of lipid accumulation compared to the administration of either compound alone. However, the results of gene expression analyses suggest that combined treatment with MACK/ORST does not lead to a synergistic interaction. Positive modulation is observed only for the expression of *sbp-1* and *mir-60*. The lack of changes in the expression of *lin-4* rather rules out a link between this microRNA and the lipid-reducing effect of MACK. The competitive interaction between the reference anti-obesity drug ORST and the natural compound MACK, which involves an overlapping molecular mechanism, is one possible explanation for the observed suppression of gene expression in nematodes treated with the hybrid combination. Accordingly, our results show that both MACK and ORST increase the expression of *sir-2.1*, whilst this effect is reduced when they are combined.

We can therefore speculate that both compounds compete for their interaction in the regulation of *sir-2.1*. The results confirm that the application of MACK, as well as its hybrid combination with ORST, increases energy expenditure in the *C. elegans-based* model of obesity and contributes to reduced lipid accumulation in both treatments. A detailed review of the signalling pathways involved reveals various molecular responses. Treatment with MACK upregulates key transcription factors and co-activators that are integral to energy expenditure and mitochondrial activity (*aak-2*, *sir-2.1*, *mdt-15*, and *nhr-49*) as well as lipid biosynthesis (*cebp-2* and *sbp-1*). On the other hand, the MACK/ORST combination primarily upregulates the expression of sbp-1 and miR-60. The results of the *in vivo* experiment not only confirm the anti-obesogenic properties of the natural pterocarpane maackiain, but also demonstrate the superior effect of maackiain compared to the control drug orlistat. Increased motility was observed in the MACK-treated group, which is an indicator of increased energy expenditure,

affecting fat accumulation in the nematodes. Mechanistically, treatment with MACK activates the molecular signalling pathways associated with calorie restriction, *aak-2/sir2.1*, and energy expenditure and lipid metabolism, *nhr-49/mdt-15*. These findings provide a rationale for further investigation into the mechanisms underlying the anti-obesogenic action of MACK and its potential use as a natural compound capable of mimicking calorie restriction.

VI. CONCLUSIONS

1. Significant anti-adipogenic activity of a ALM extract has been established through its influence on the PI3K/AKT signalling pathway in human adipocytes.
2. Quercitrin significantly suppresses lipid accumulation, whilst lipolysis is moderately inhibited.
3. The anti-adipogenic activity of OSR extract is due to its indirect influence on the molecular pathways responsible for adipogenic differentiation .
4. Ononin demonstrates anti-adipogenic activity by regulating SIRT1 and inhibiting PPARγ.
5. Maackiain inhibits adipogenesis *via* PPARγ signalling and suppresses lipogenesis by downregulating SREPB1 and the lipogenic genes it regulates.
6. The potential of maackiain to inhibit lipid metabolism has been confirmed for the first time at the organismal level in *C. elegans*.

VII. CONTRIBUTIONS

With fundamental and scientific character:

1. The potential of *Alchemilla monticola* Opiz extract to inhibit differentiation and lipid accumulation in human adipocytes has been revealed, as well as the role of its active components astragalin and quercitrin.
2. The effect of *A. monticola* extract in suppressing the early stage of adipogenesis in human adipocytes by inhibiting PI3K activity has been determined.
3. The modulated signalling pathway responsible for the observed anti-adipogenic effect of *A. monticola* extract has been identified, namely the PI3K/AKT pathway and PPARγ protein levels.
4. The bidirectional effect of astragalin on the regulation of the PI3K/AKT signalling pathway in human adipocytes has been established, with the critical concentration for this bidirectional regulation being between 10-25 μM.
5. The potential of maackiain to inhibit adipogenesis *via* PPARγ/C/EBPα signalling, and lipogenesis *via* downregulation of SREBP1 and its lipogenic genes, has been demonstrated.
6. A proposed mechanism of action for the anti-adipogenic effect of ononin involves the upregulation of SIRT1 and the inhibition of PPARγ.
7. The potential of maackiain to activate the molecular signalling pathways associated with calorie restriction (*aak-2/sir2.1*) and energy expenditure and lipid metabolism (*nhr-49/mdt-15*) has been demonstrated in an *in vivo* model.

Scientific and applied significance:

The data obtained suggest that maackiain could be used as a natural compound capable of mimicking calorie restriction.

Acknowledgements

I would like to express my sincere gratitude to:

- Prof. Dr Milen I. Georgiev, my scientific supervisor – for the trust and his advice regarding the experimental work and the interpretation of the results, as well as for the discussions on the preparation of the thesis.
- My colleagues from the Metabolomics Laboratory team at the "Stefan Angeloff" Institute of Microbiology, Bulgarian Academy of Sciences, Plovdiv, and the Center for Plant and Systems Biology and Biotechnology, Plovdiv, for their assistance in carrying out the analyses, processing the results, and discussing the data obtained, as well as for their support and dedication in the completion of this thesis.
- The management of the "Stefan Angeloff" Institute of Microbiology for their institutional support.
- My family and friends for their continuous support and encouragement.

The scientific research included in this thesis was carried out with the financial support of the PlantaSYST project (SGA No 739582 and FPA No. 664620) under the European Union's Horizon 2020 programme, and project BG05M2OP001-1.003-001-C01, funded by the European Regional Development Fund through the 'Science and Education for Smart Growth' operational programme.

Published materials on the dissertation

Scientific publications

1. **Mladenova, S.**, Todorova, M., Savova, M., Georgiev, M.I., Mihaylova, L. 2023. Maackiain mimics caloric restriction through *aak*-2-mediated lipid reduction in *Caenorhabditis elegans. International Journal of Molecular Sciences* 24(24), 17442 (**IF_{2023} 4.9, Q1**).
2. **Mladenova, S.,** Savova, M.S., Marchev, A.S., Ferrante, C., Orlando, G., Wabitsch, M., Georgiev, M.I. 2022. Anti-adipogenic activity of maackiain and ononin is mediated *via* inhibition of PPARγ in human adipocytes. *Biomedicine and Pharmacotherapy* 149, 112908 (**IF_{2022} 7.5, Q1**).
3. **Mladenova, S.**, Vasileva, L., Savova, M.S., Marchev, A., Tews, D., Wabitsch, M., C. Ferrante, C., Orlando, G., M. Georgiev, M.I. 2021. Anti-adipogenic effect of *Alchemilla monticola* is mediated *via* PI3K/AKT signaling inhibition in human adipocytes. *Frontiers in Pharmacology* 12, 707507 (**IF_{2021} 5.988, Q1**).

Total impact factor (IF): 18.388

Participation in scientific conferences

Oral reports

1. Savova M.S., Todorova M.N., Mladenova S.G., Binev B.K., Georgiev M.I., Mihaylova L.V. 2025 Cross-talk between PI3K/AKT/GSK3 and AMPK/SIRT1 signaling pathways in the development of obesity and metabolic disorders. *6th International Conference on Natural Products Utilization: from Plants to Pharmacy Shelf*, 27-30 May Bansko, Bulgaria.
2. Mihaylova, L., Savova, M., Todorova, M., **Mladenova, S**., Proikova, N., Balcheva-Sivenova, Z., Georgiev, M.I. 2023. Integrating Molecular Pharmacology for Accelerated Discovery of Anti-Obesity Natural Molecules. *VIII Congress of Pharmacy with International Participation,* April 27-30, Borovets, Bulgaria.
3. Georgiev, M.I., Savova, M.S., Mladenova, S. 2022. Anti-obesity molecules of natural origin. *11th Conference on Medicinal and Aromatic Plants of Southeast European Countries*, 6-10 October, Ohrid, Republic of North Macedonia.
4. Vasileva, L., Savova, M., **Mladenova, S**., Amirova, K., Blacheva-Sivenova, Z., Georgiev, M.I. 2021. Human adipocytes react with browning upon caffeic and chlorogenic acids co-treatment. *1st International Conference on Plant Systems Biology and Biotechnology*, 14-17 June, Golden Sands Black Sea resort, Bulgaria.

Poster pesentations

1. **Mladenova, S.**, Savova, M., Mihaylova, L., Todorova, M., Georgiev, M.I. 2023. Maackiain restricts lipid accumulation in glucose-fed *Caenorhabditis elegans*. *5th International Conference on Natural Products Utilization*, 30 May - 2 June 2023, Sts. Constantine and Helena Resort, Bulgaria.
2. Mihaylova, L., **Mladenova, S**., Savova M., Balcheva-Sivenova, J., Marchev, A., Georgiev M.I. 2022. PPARγ inhibition mediates *Alchemilla monticola* Opiz anti-adipogenic effect in human adipocytes. *11th Conference on Medicinal and Aromatic Plants of Southeast European Countries*, 6-10 October, Ohrid, Republic of North Macedonia.
3. **Mladenova, S.,** Vasileva, L, Savova, M., Marchev, A., Koycheva, I., Georgiev, M.I. 2021. Astragalin and quercitrin exert anti-obesity potential through PPARγ-mediated mechanism. *1st International Conference on Plant Systems Biology and Biotechnology*, 14-17 June, Golden Sands Resort, Bulgaria.